



Classification and mineralization of global lithium deposits and lithium extraction technologies for exogenetic lithium deposits

Mian-ping Zheng^{a,*}, En-yuan Xing^{a,*}, Xue-fei Zhang^a, Ming-ming Li^b, Dong Che^a, Ling-zhong Bu^a, Jia-huan Han^b, Chuan-yong Ye^a

^a Key Laboratory of Saline Lake Resources and Environment (Ministry of Natural Resources), Institute of Mineral Resources, Chinese Academy of Geological Sciences, Beijing 100037, China

^b China University of Mining and Technology (Beijing), Beijing 100083, China

ARTICLE INFO

Article history:

Received 26 June 2023

Received in revised form 8 August 2023

Accepted 7 September 2023

Available online 16 October 2023

Keywords:

Exogenetic lithium deposit

Endogenetic lithium deposit

Deposit type

Salt lake type

Deep brine type

Geothermal type

Volcanic deposit type

Clay type

Supernormal supergene enrichment

SGSP lithium extraction technology

Invention patent

Mineral resource exploration engineering

ABSTRACT

A reasonable classification of deposits holds great significance for identifying prospecting targets and deploying exploration. The world's keen demand for lithium resources has expedited the discovery of numerous novel lithium resources. Given the presence of varied classification criteria for lithium resources presently, this study further ascertained and classified the lithium resources according to their occurrence modes, obtaining 10 types and 5 subtypes of lithium deposits (resources) based on endogenetic and exogenetic factors. As indicated by surveys of Cenozoic exogenetic lithium deposits in China and abroad, the formation and distribution of the deposits are primarily determined by plate collision zones, their primary material sources are linked to the anatectic magmas in the deep oceanic crust, and they were formed primarily during the Miocene and Late Paleogene. The researchers ascertained that these deposits, especially those of the salt lake, geothermal, and volcanic deposit types, are formed by unique slightly acidic magmas, tend to migrate and accumulate toward low-lying areas, and display supernormal enrichment. However, the material sources of lithium deposits (resources) of the Neopaleozoic clay subtype and the deep brine type are yet to be further identified. Given the various types and complex origins of lithium deposits (resources), which were formed due to the interactions of multiple spheres, it is recommended that the mineralization of exogenetic lithium deposits (resources) be investigated by integrating tectono-geochemistry, paleoatmospheric circulation, and salinology. So far, industrialized lithium extraction is primarily achieved in lithium deposits of the salt lake, clay, and hard rock types. The lithium extraction employs different processes, with lithium extraction from salt lake-type lithium deposits proving the most energy-saving and cost-effective.

©2023 China Geology Editorial Office.

1. Introduction

To achieve the goal of carbon neutrality, promoting the development of new energy has become a global consensus. Lithium is known as a new energy metal from the perspective of resources. With the rapid development of new energy vehicles and mobile energy storage equipment, lithium has become a strategic mineral that is highly valued by countries

across the world. The geological resource prospecting of lithium has become a popular research topic, and the research on the origin and mineralization types of lithium resources has contributed to a significant increase in global lithium resources. For example, research on the pyroclastic clay-subtype lithium deposits (resources) has increased the metallic lithium resources of the U.S. from 35000 tons in 2019 to 630000 tons in 2020 and then to 1000000 tons in 2023, indicating a surge by over 28 times in just four years (USGS, 2019; USGS, 2020; USGS, 2021; USGS, 2022; USGS, 2023).

2. Classification of global lithium deposits

A reasonable classification of deposits is critical for understanding the essence of mineralization, identifying prospecting targets and focus, and effectively deploying

First author: E-mail address: zhengmp2010@126.com (Mian-ping Zheng).

* Corresponding author: E-mail address: zhengmp2010@126.com (Mian-ping Zheng); xingenyuan2022@126.com (En-yuan Xing).

Literary editor: Xi-jie Chen

doi:10.31035/cg2023061

2096-5192/© 2023 China Geology Editorial Office.

exploration. Previously, lithium deposits were primarily classified into the salt lake and hard rock types. Driven by a surge in demand for lithium resources and an increase in the diversity of lithium resources, some novel lithium resources have been discovered. Given the presence of varied classification criteria for lithium resources presently, it is necessary to further define and classify lithium resources based on their occurrence characteristics. This study classified lithium deposits (resources) into endogenous and exogenous lithium deposits (resources). The former, formed either by magmatism or in gasification and hydrothermal processes, occurs at a certain burial depth under high temperatures and pressure. The latter, formed by exogenic mineralization on the Earth's surface, refers to lithium deposits (resources) formed

after ore-forming materials migrate and accumulate *via* the action of solar energy, as well as interactions of the lithosphere with the hydrosphere, atmosphere, and biosphere, under low temperatures and pressures near the surface (Table 1; Fig. 1).

Exogenous lithium deposits: salt lake type (consisting of salt-lake brine subtype and salt-lake solid carbonate subtype), deep brine type, geothermal type, volcanic deposit type (Jadarite [$\text{LiNaSiB}_3\text{O}_7(\text{OH})$]), and clay type (comprising pyroclastic clay subtype, silico-aluminous clay subtype, and coal-measure subtype).

Endogenous lithium deposits: pegmatite type, granite type, greisen type, magmatic-hydrothermal type, and volcanic cryptoexplosion type.

Table 1. Classification of the world's primary lithium resources.

Genetic type		Research and exploitation degrees		Typical deposits
Exogenous	Salt lake type	Salt-lake brine subtype	High research and exploitation degrees	Altiplano Lithium Triangle (the Uyuni, Atacama, and Hombre Muerto salt lakes) in Andes, South America; salt lakes on China's Qinghai-Tibet Plateau; salt lakes in southwestern U.S.
		Solid carbonate subtype	First discovered in the Zabuye Salt Lake, Tibet, China, with the lithium resources having been reported	Zabuye Salt Lake in northern Tibet, China
	Deep brine type	Great potential but a low research degree	Cenozoic tectonic zone in the western Qaidam Basin, China; deep Triassic brine in Huangjinkou, Xuanhan, Sichuan Basin, China; Smackover deposit in Arkansas, U.S.; Alberta, Canada	
	Geothermal type	Unclear potential, restricted by the progress in exploration technology and efforts	The Moluo River and Semi geothermal water in Tibet; Brawley and Salton in southern California, U.S.	
	Volcanic deposit type	Jadarite [$\text{LiNaSiB}_3\text{O}_7(\text{OH})$]	Formed in Miocene volcanic deposits, with exploration roughly completed and entering the mining stage	Superlarge lithium-boron deposits in the Jadar Basin, Serbia
	Clay type	Pyroclastic weathered clay subtype	Deposits formed by the weathering and lithium enrichment of lithium-bearing pyroclastic rocks, with a few (in western Silver Peak Lake) exploited and utilized earlier	Kings Valley in Nevada, U.S.—a valley in a plateau in south-central Mexico
		Silico-aluminous clay subtype (potential resources)	Formed during the Neopaleozoic and extensively distributed, with a low exploration degree (still in a pioneering stage)	The Dazhuyuan deposit in Guizhou, China
	Coal-measure clay subtype (potential resources)	Extensively distributed, with a low exploration degree (still in a pioneering stage)	The Jungar coal field in China, the Ningwu coal field in Shanxi, China	
Endogenous	Granite pegmatite type	High grades and having been extensively surveyed	The Greenbushes lithium deposit in Australia; the Altay deposit in Xinjiang, China; the Jiajika and Maerkang deposits in Sichuan, China	
	Granite type	Low grades, requiring high exploitation and utilization costs	Deposits in China, including the No. 414 deposit in Jiangxi, the Zhengchong and Jianfengling deposits in Hunan, and the Limu deposit in Guangxi	
	Greisen type	Low grades, requiring high exploitation and utilization costs	The Tréguennec and Ezi deposits in France; the Zhengchong deposit in Xiangyuan, Daoxian County, Hunan Province, China	
	Magmatic-hydrothermal type	Low grades, requiring high exploitation and utilization costs	The Mahuaping deposit in the Sanjiang area, southwestern China	
	Volcanic cryptoexplosion type	Low exploitation degrees	The Weila Situo deposit in Inner Mongolia, China, distributed primarily in the volcanic cryptoexplosive pipes and their surrounding quartz veins, with lithium-bearing minerals primarily including lepidolites	

(Data source: Zheng MP et al., 1989a, b; Zhao YY et al., 2015; Wang DH et al., 2013; Li JK et al., 2014; Li BY et al., 2018; Shu LS et al., 2021)

Exogenetic lithium deposits can be divided into solid and liquid phases, including two types of liquid lithium deposits (deep brine type, geothermal type), two types of solid lithium deposits (volcanic deposit type, clay type), and one type of both solid and liquid lithium deposits (salt lake type).

2.1. Salt lake type

2.1.1. Salt-lake brine subtype

Lithium deposits of this type contribute above 60% of the global lithium resource reserves. Owing to their relatively low exploitation costs and environmental friendliness, salt-lake brine-subtype lithium deposits serve as a primary type of lithium deposits to be exploited in the world. Salt lake-type lithium resources primarily occur in brine, with lithium grades reaching the industrial recoverable grade. Relevant Chinese standards stipulate that the minimum industrial grade and cut-off grade of LiCl are 300 mg/L and 150 mg/L, respectively. Lithium-bearing brine in salt lakes tends to coexist with sodium, potassium, boron, and even rubidium, cesium, and bromine.

2.1.2. Solid carbonate subtype

Despite rare solid lithium in lithium-bearing salt lakes, natural lithium carbonate (including zabuyelite and lithium-bearing dolomite, Fig. 2) was first found in a carbonate-type salt lake in Tibet, China (Zheng MP et al., 1987), suggesting the discovery of a new type of lithium carbonate deposit. This type of lithium deposit is primarily composed of natural lithium carbonate and lithium-bearing dolomite^① (Zheng MP et al., 1987). Presently, this type of lithium deposit is mainly found in salt lakes, such as the Zabuye Salt Lake in northern Tibet, China. As revealed by detailed surveys and investigation through drilling, the lithium deposits in the Zabuye Salt Lake consist predominantly of two industrial types of ores: halite-lithium ores and double salt–lithium ores. With indices of the solid salt deposits exceeding those of general deposits, the lithium deposits in the Zabuye Salt Lake have yielded satisfactory lithium extraction results. As per the requirements of the National Committee on Mineral Reserves of China (the former of the National Commission of Mineral Resources), the authors of this study proposed the industrial indices of the deposit, which have been approved by the Ministry of Natural Resources of the People's Republic of China (GTZH (2001) No. 394; Table 2). This deposit boasts 1.022 million tons of Li₂CO₃ resources and reserves, including 0.102 million tons of reserves^①.

Solid carbonate-subtype lithium deposits may also occur in other lithium-bearing carbonate salt lakes. In addition, sulfate-type salt lakes may produce lithium-bearing double salts such as lithium-sodium sulfates.

2.2. Deep brine type

This type of lithium resource has been found in China, the

U.S., and Canada. It is preliminarily estimated that the Paleogene and Neogene strata in the Nanyishan area in the western Qaidam Basin and the Triassic strata in Sichuan have lithium-bearing deep brine resources of 6.4 million tons of LiCl. In five states of the U.S. (including Arkansas), all deep brine (oil field water) bears lithium. For instance, the brine in the Smackover Formation in the south-central gulf area in the U.S. has a lithium content of up to 692 mg/L (Garrett DE, 2004), with resource evaluation having been conducted. The lithium-bearing deep brine (oil field water) in the western Qaidam Basin, distributed in desert areas, with low Mg/Li ratios, has been investigated for many years. Presently, organizations such as the Salt Lake Center of the Institute of Mineral Resources have conducted exploration and scaled-up salt pan experiments cooperating with the Qinghai Oil Field.

So far, this type of lithium deposit has received extensive concern from the global lithium industry. Such lithium deposits refer specifically to deep brine (oil field water) with high lithium content, commonly mixed with oil and gas. Given that there is no available evaluation index for lithium content in deep brine, the evaluation indices for salt-lake brine are presently used instead. Moving forward, because of the different geographical, economic, and technical conditions of this type of lithium deposits, it is necessary to conduct scaled-up process tests and consider local conditions when formulating economic and practical specifications.

2.3. Geothermal type

Geothermal lithium deposits are a new type of lithium resources for which exploration has commenced recently. Most of the lithium-bearing geothermal water in the world, such as the Qinghai-Tibet Plateau, the Lithium Triangle in South America, and the Salton Sea geothermal area in North America, is genetically related to the above-mentioned three types of lithium deposits. The geothermal water and lake water in the Salton Sea geothermal area display lithium concentrations of 9×10^{-6} – 93×10^{-6} and 152×10^{-6} – 209×10^{-6} , respectively. Industrial lithium extraction from geothermal water has commenced in this geothermal area by Simbol, Inc. It has been reported that a large amount of geothermal water has a lithium content of 54–126 mg/L in South America. Along the Yarlung Zangbo high-temperature geothermal field in Tibet, the authors of this study have identified 15 sites of geothermal water resources with lithium grades approximating or reaching the cut-off grade and minimum industrial grade of lithium. These geothermal water resources have lithium content between 20–239 mg/L and exceeding 35 mg/L in geothermal water in the Moluo River, Semi, Zhumoshu, and Riruofeishui (Zheng MP et al., 1995; Wang CG et al., 2019).

Exogenetic lithium deposits of the solid phase can be classified into the Jadarite type, clay type, and solid carbonate subtype.

^①Zheng MP, Yang Q, Yin ZY, Liu XF, et al., 2022. Report on the detailed survey of lithium and potassium in the lithium deposit in the Zabuye Salt Lake, Tibet (an internal report).

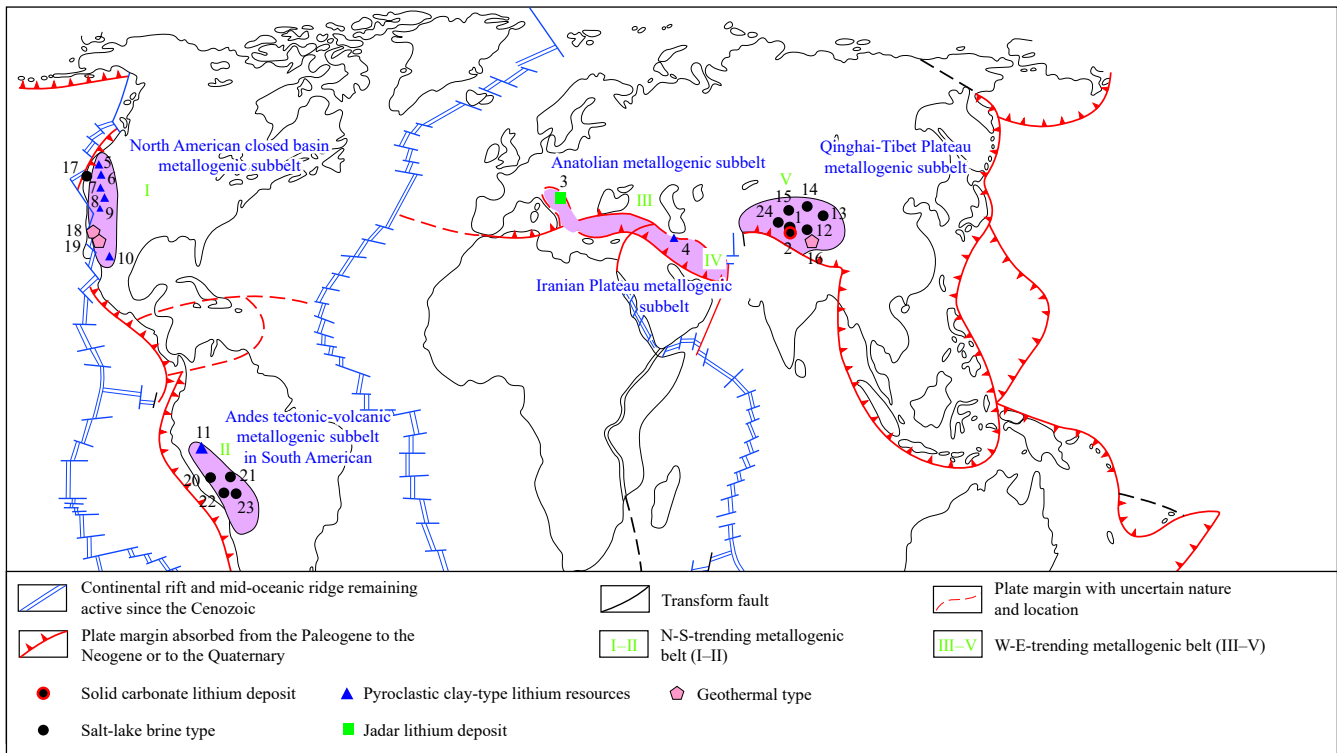


Fig. 1. Schematic diagram showing the zonation and distributions of global Cenozoic exogenetic lithium resources (the tectonic setting cited from O3OJI, 1987). 1–Solid carbonate deposit in the Zabuye Salt Lake; 2–Brine-type lithium deposit in the Zabuye Salt Lake; 3–Jadar lithium deposit; 4–Iranian lithium resources; 5–Big Sandy lithium resources; 6–Silver Peak lithium resources; 7–Northern Clayton lithium resources; 8–Tonopah lithium resources; 9–Thacker Pass lithium resources; 10–Sonora lithium resources; 11–Falchani lithium resources; 24–Chagcam Caka Salt Lake in Tibet; 12–Dangxiogcuo Salt Lake in Tibet; 13–Qarhan Salt Lake in Qinghai; 14–East and west Jinaier salt lakes in Qinghai; 15–Yiliping Salt Lake in Qinghai; 16–Semi in Tibet; 17–Death Valley in the U.S.; 18–Brawley, California, the U.S.; 19–Salton, California, the U.S.; 20–Peru salt lake group; 21–Coipasa Salt Lake, Bolivia; 22–Uyuni Salt Lake, Bolivia; 23–Atacama Salt Lake, Chile .

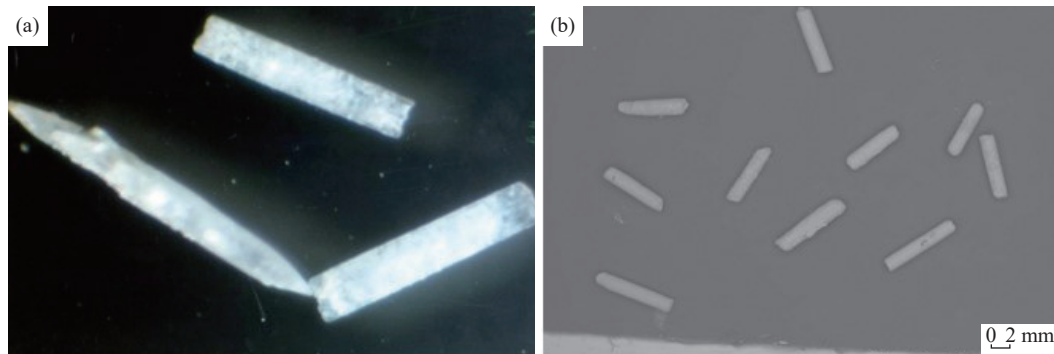


Fig. 2. Microscopic images of lithium-bearing carbonate minerals at Zabuye. a–Zabuyelite (Li_2CO_3); b–Lithium-bearing dolomite (lithium concentration: 1750×10^{-6}) at Zabuye .

Table 2. Industrial indices of solid lithium deposits.

Cut-off grade/%	Minimum industrial grade/%	Recoverable thickness/m	Band rejected thickness/m
LiCl 0.11 (including 0.096 for Li_2CO_3)	≥ 0.34 (including 0.296 for Li_2CO_3)	0.5	0.5

2.4. Volcanic deposit type (Jadarite)

This type of lithium deposit is typified by a special superlarge lithium-boron deposit discovered in the Jadar Basin, Serbia (“Jadar lithium deposit”). The ore mineral of this deposit is dominated by jadarite [$\text{LiNaSiB}_3\text{O}_7(\text{OH})$] with 47.2% B_2O_3 and 7.2% Li_2O – a unique mineral bearing lithium and boron in the world. The ore-prospecting indicator

of this deposit is the tuff layer in Miocene lacustrine volcanic sedimentary rocks, which boasts Li_2O resources of around 2.06 million tons and B_2O_3 resources of approximately 15 million tons (Zhao YY et al., 2015; Liu LJ et al., 2017).

Jadarite, a new mineral (2006-36) approved by the International Mineralogical Association, represents a new type of lithium (boron) deposit (Stanley CJ et al., 2007). However, Benson TR et al. (2017) classified the Jadar lithium

deposit as a clay-type deposit, and Bradley TR et al. (2017) referred to it as a lithium-zeolite deposit. The two classifications are inappropriate since the Jadar lithium deposit is composed of neither lithium-bearing clays nor lithium-bearing zeolites.

Given that jadarite is a homogeneous lithium- and boron-bearing mineral rather than a clay mineral, this mineral is classified as a new type in this study.

2.5. Clay type

Since the 1970s, the U.S. has discovered clay-type lithium resources in McDermitt Caldera, evidenced by the facts that Vine JD and Dooley JR (1980) termed these resources “lithium-clay deposits” in their report in 1980, and Ferrell JE (1985) termed them “lithium-bearing clays” in his report in 1985. These terms appropriately reflect the mineral composition of sedimentary rocks in this type of lithium resource. However, Gruber PW et al. (2011) and Christmann P et al. (2015) divided lithium deposits into only three to four types, classifying the lithium resources with sedimentary origin (e.g., clay-type lithium deposits) as sedimentary rocks or sediment-hosted deposits. This classification might lead to confusion between clay-type lithium deposits and other salt-lake- and geothermal-type lithium-bearing sediments in future surveys.

Many Chinese researchers have been misled by the inappropriate use of terms and expressions by some foreign scholars. As a result, some of them commonly use the term “sedimentary-type lithium deposits” to represent all lithium-bearing clay deposits (Wu XS et al., 2014; Wang QS et al., 2015; Liu LJ et al., 2017; Yu F et al., 2019; Zhang YL et al., 2022). Given that the terms for lithium deposit types used by some scholars at home and abroad deviate from the fundamental conception of sedimentology, it is necessary to correct related terms for lithium-bearing clay types.

The authors of this study suggest that lithium deposits (resources) hosted in pyroclastic sedimentary strata, bauxites, and coal measures should be further classified into subtypes of pyroclastic weathered, silico-aluminous, and coal-measure clay.

2.5.1. Pyroclastic weathered clay subtype

The ore-hosting surrounding rocks of this subtype of lithium deposit are dominated by pyroclastic rocks, such as tuffs and tuffites. The pyroclasts in them, originating from Miocene craters, formed lacustrine lithium-bearing clay sediments in the later stage followed by weathering and leaching. The ore-forming materials and dynamics of this subtype of lithium deposits primarily originated from volcanism.

The lithium resources of this subtype are typified by the Thacker Pass lithium deposit situated at the junction of the Nevada and Oregon states of the U.S. This deposit is found within an oval paleocrater named McDermitt Caldera, which is about 40 km long from north to south and 30 km wide from east to west (Benson TR et al., 2023). This crater, formed at

16.30 Ma, is associated with the hot spot over the mantle plume in the Yellowstone area. Over the hundreds of thousands of years after volcanic eruptions, water infiltrated into volcanic rocks, leaching out lithium elements. These lithium elements were deposited in the crater basin, forming a crater lake and many related lacustrine sediments. As the crater was elevated by the Pleistocene volcanic activity, the lake water was expelled, carrying lithium-rich sediments to the surface. As released in June 2018: (1) with 2500×10^{-6} as the cut-off grade, it can be estimated that the Thacker Pass lithium deposit has lithium resources of 179.422 million tons and an average grade of 3283×10^{-6} , equivalent to about 3.135 million tons of lithium carbonate; (2) with 2000×10^{-6} as the cut-off grade, it is estimated that this deposit has lithium resources of 385.26 million tons and an average grade of 2917×10^{-6} , equivalent to approximately 5.982 million tons of lithium carbonate (Yu F et al., 2019).

Therefore, lithium deposits of this subtype experienced initial accumulation in the endogenetic stage. However, this stage did not witness lithium mineralization, which occurred only under supergene conditions. These lithium deposits have been utilized. In contrast, breakthroughs have not been made in the exploitation and utilization of the other two clay subtypes of lithium deposits. Recently, great progress has been made in the exploration and exploitation of pyroclastic clay-subtype lithium resources, with the U.S. having seen a significant increase in resources of these lithium resources. Due to the inherent lack of high-quality lithium-bearing salt lakes and hard-rock lithium in the U.S., the geological sector and enterprises of this country attach great importance to research on the Cenozoic volcanic deposits and the Lithium Triangle, aiming to expand their domestic lithium resources. In 2018, the American Geophysical Union (AGU) held a meeting on strategic mineral lithium, inviting lithium resource scientists from all over the world to research and exchange views on the expansion of lithium resource types (AGU, 2018). From 2018 to 2020, North American countries (e.g., the U.S. and Mexico) also made significant progress in prospecting and evaluating pyroclastic clay-subtype lithium deposits.

2.5.2. Silico-aluminous clay subtype

For this subtype of lithium deposits, the ore-hosting surrounding rocks primarily comprise clays, aluminous clays, and bauxites, containing minor amounts of clastic rocks (i.e., shales, siltstones, fine-grained sandstones, and coarse-grained sandstones). Their ore-forming materials and dynamics are associated with weathering. The Benxi Formation in Shanxi Province exhibits a lithium content of up to 1.916%–1.909% (Chen P, 1997). Typical silico-aluminous clay-subtype lithium resources include the Dazhuyuan bauxite deposit in Guizhou. This deposit, spanning Wuchuan, Zheng'an, and Daozhen counties and adjoining Chongqing, is the most representative bauxite deposit in the region. Wang DH et al. (2013) analyzed 81 samples from borehole cores in the Dazhuyuan bauxite deposit, finding that 61 samples exhibited

lithium contents of over 260×10^{-6} , with an average of 741×10^{-6} . Additionally, they discovered that continuously distributed ore-bearing strata with lithium content exceeding 600×10^{-6} are up to several meters thick in some boreholes.

2.5.3. Coal-measure clay subtype

Lithium deposits paragenetic and associated with coals (coal measures) can form when the lithium content in coals exceeds a certain grade. Although most coal measures exhibit relatively low metal content, lithium resources may still form in coal seams under specific geological conditions, with grades equivalent to or even higher than that of traditional lithium deposits (Zhao L et al., 2022). Typical coal-measure clay-subtype lithium resources include the No. 6 coal seam in the Junggar coal field. This coal seam boasts about 24 billion tons of coal reserves, accounting for two-thirds of the total reserves of the coalfield, with a lithium content of 147×10^{-6} . As calculated based on this, the prospect resources of the No. 6 coal seam can reach 3.528 million tons of Li_2O (Yu F et al., 2019). The Late Triassic coals in Chongqing boast Li_2O resources of 1.3069 million tons, as calculated based on the average high-temperature ash yield of 29.12% and coal resources of 2.083 billion tons (Zhao L et al., 2022).

3. Mineralization of exogenetic lithium deposits

3.1. Distributions of Cenozoic exogenetic lithium deposits

The distributions of global Cenozoic exogenetic lithium (boron, rubidium, and cesium) deposits are dictated by plate collision zones, forming two major intercontinental giant metallogenic belts (Fig. 1): and N-S- and W-E-trending metallogenic belts. The former consists of the North America southwestern basin metallogenic subbelt I and the South America plateau metallogenic subbelt II, while the latter comprises the Anatolia metallogenic subbelt III, the Iranian Plateau metallogenic subbelt IV, and the Qinghai-Tibet Plateau metallogenic subbelt V (Zheng MP et al., 2016, 2018). In terms of the scale of lithium-bearing salt lakes, the South America plateau metallogenic subbelt II, the Qinghai-Tibet Plateau metallogenic subbelt V, and the North America southwestern basin metallogenic subbelt I outperform other subbelts. In terms of the hydrochemical type, zonation, and mineral composition of exogenetic lithium-bearing salt lakes, the Qinghai-Tibet Plateau metallogenic subbelt V exhibits superior diversity and zonation among the three metallogenic subbelts. China has made remarkable progress in the exploration and exploitation of Cenozoic exogenetic lithium deposits through large-scale surveys over six decades.

As revealed by a study on the lithospheric evolution of Altiplano fault zones in Andes (McQuarrie N et al., 2005), the lithium in the N-S-trending metallogenic belt of exogenetic lithium deposits in lithium-bearing salt lakes originated from the surface argillaceous sediments in the Western Pacific Ocean and magmatic rocks formed by mantle remelting. This finding suggests that global lithium-bearing salt lakes display

supernormal enrichment characterized by deep sources and exogenetic mineralization under the Late Cenozoic active tectonic setting.

3.2. Material sources of exogenetic lithium deposits

The above-mentioned studies show that the Cenozoic exogenetic lithium deposits are intimately related to the Neogene and later volcanic deposits (especially volcanic ash), as well as their carrier geothermal water (hydrothermal fluids).

3.2.1. Contribution of volcanic tuffs to exogenetic lithium-forming process

The Neogene volcanic rocks (trachytes, rhyolites, and tuffs) found in lithium triangle regions all originated from anatexic magmas, thus exhibiting higher lithium content than ordinary volcanic rocks. So far, it has been found that the lithium in lithium-bearing salt lakes occurs in various forms, including lithium-bearing brine in salt sediments of salt lakes and that in lacustrine clastic rocks.

In 1987, the authors of this study witnessed mine workers using hot water (and a small amount of hydrochloric acid, as learned later) to dissolve the brine within the lithium-bearing tuff clay layers in the Silver Peak Lake in Nevada, the U.S. The dissolved brine was then pumped into the modern salt pans of the Silver Peak Lake to serve as an additional raw material source for lithium production. The Miocene volcanic tuffaceous lacustrine sediments surrounding the basin of the Silver Peak Lake have lithium contents of up to 1300×10^{-6} , with an average of 100×10^{-6} (Kunasz IA, 1974; Davis JR et al., 1979). The study on the lithium source of the Salar de Diablillos and surrounding lithium-containing salt lakes in Argentina also indicates that most of the lithium in the salt lakes comes from the peripheral volcanic tuff rocks. (Sarchi C et al., 2023)

3.2.2. Contribution of lithium-bearing hydrothermal fluids to lithium-forming process in lakes

During the late post-collision period of the Qinghai-Tibet Plateau [the Early Miocene (N_1^1 , 21–15 Ma)], the plateau underwent a significant uplift. Due to this uplift, accompanied by lithium mineralization, highly volatile dilute alkali and boron formed volcanic flows upward and then erupted to the surface, forming volcanic deposits with lithium contents of up to 85×10^{-6} – 150×10^{-6} . Large-scale weathering and leaching of Early Miocene lithium- and boron-rich volcanic deposits produced large quantities of lithium-bearing materials to recharge the nearby salt lake area (Fig. 3).

Extensive travertine spreads across the Miocene volcanic deposits in the Qinghai-Tibet Plateau. travertine cones are widely exposed at elevations of 4625–4675 m in the Xiongba area, with areas ranging from tens of square meters to 2 km^2 and lithium and boron contents varying as follows from 24–135 ka BP (Table 3).

Due to large-scale ancient and modern geothermal water

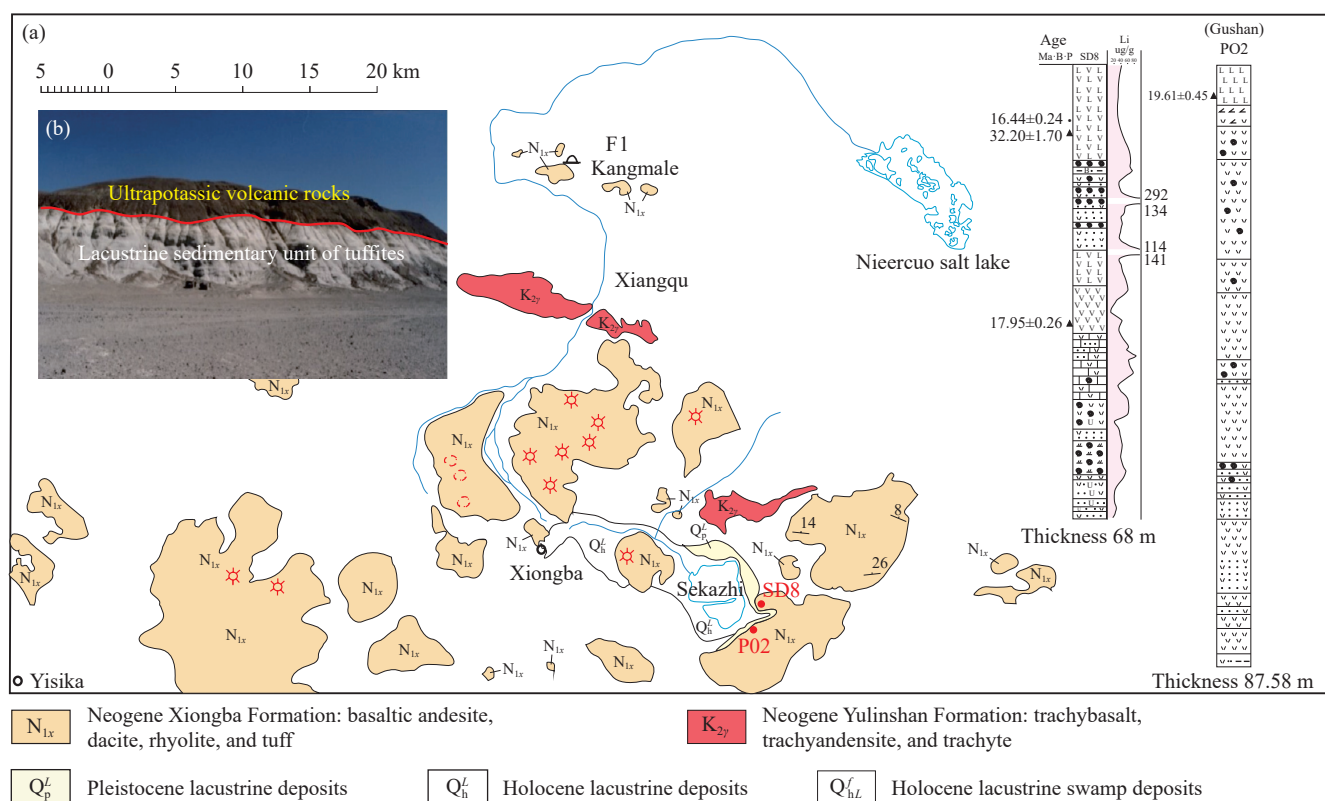


Fig. 3. Distribution and profiles of volcanic deposits in the Sekazhi area^①.

activity along the fault system on the plateau, significant quantities of lithium-bearing hydrothermal fluids upwelled. As a result, massive lithium-bearing geothermal water and lithium-rich travertine and geysirite accumulate on the surface. In the lithium ore concentration area of the Zabuye Salt Lake, travertine that upwelled to the surface are widely distributed (Fig. 4) from the modern lake bottom to the ancient lake surface.

In the basin of the Zabuye Salt Lake, extensive ancient travertine accumulate in the central part of and on the western bank of the lake, forming the Zabuye travertine island in the lake center. The travertine island, connected to the inter-lake gravel dam, divides the lake into the south and north lakes. Hundreds of white travertine cones are scattered in the north lake, either exposed or submerged under water, with top surface areas ranging from several to dozens of square meters. Presently, a small amount of low-temperature thermal spring water is still gushing out, with an average lithium content of 2 mg/L. The numerous travertine in the Zabuye travertine island result from the large-scale geothermal water recharge along the fault system over a prolonged period (Zheng MP et al., 1989b). Until now, low-temperature thermal spring water still exists (23°C in winter), with a water yield of 50000 m³/d and lithium content of 5 mg/L.

In 2020, the authors first discovered geysirite under the Zabuye travertine island (Fig. 5). These deposits display various mineral textures such as spherical and breccia cemented textures, suggesting that significant water activity like explosion carried numerous deep lithium-bearing substances (Fig. 6). The analysis shows that ancient geysirite

Table 3. Lithium and boron content in travertine in the Xiongba area (24–135 ka BP).

Sample No.	Li/×10 ⁻⁶	B/×10 ⁻⁶	Age/A.D.
NEG2015	6.61	4.93	23981±803
NEG2019	6.41	4.77	39660±2344
NEG2022	3.10	2.75	134946±1277

(1709±146 ka to 2821±206 ka) prevails the travertine island, still preserving lithium anomalies inside (22×10⁻⁶–33×10⁻⁶).

Based on the lithium content, distribution area, and age (about 140 ka) of existing travertine, as well as the lithium content in the lake area recharged by modern thermal spring water, it can be estimated that the ore concentration area at Zabuye has supplied approximately 100 million tons of metal lithium (geochemical amount) to the surface.

3.3. Supergene supernormal enrichment of lithium

3.3.1. Distribution of salt lake resources in the Qinghai-Tibet Plateau

The Qinghai-Tibet Plateau boasts considerable salt lake resources (Fig. 7). This plateau remained a slightly warm humid climate of the south temperate zone, with drought periods present locally, from the Miocene until the Middle Pleistocene (132 ka BP), when it still exhibited a climate with alternating slightly warm humid features and dry and cold features. As a result, five greatest lake periods were formed: roughly 132–112 ka BP, 110–95 ka BP, 91–72/83–75 ka BP, 65–53 ka BP, and 40–30/40–35 ka BP (Zheng MP et al., 2006). With the thriving and dying of big lakes, large-scale

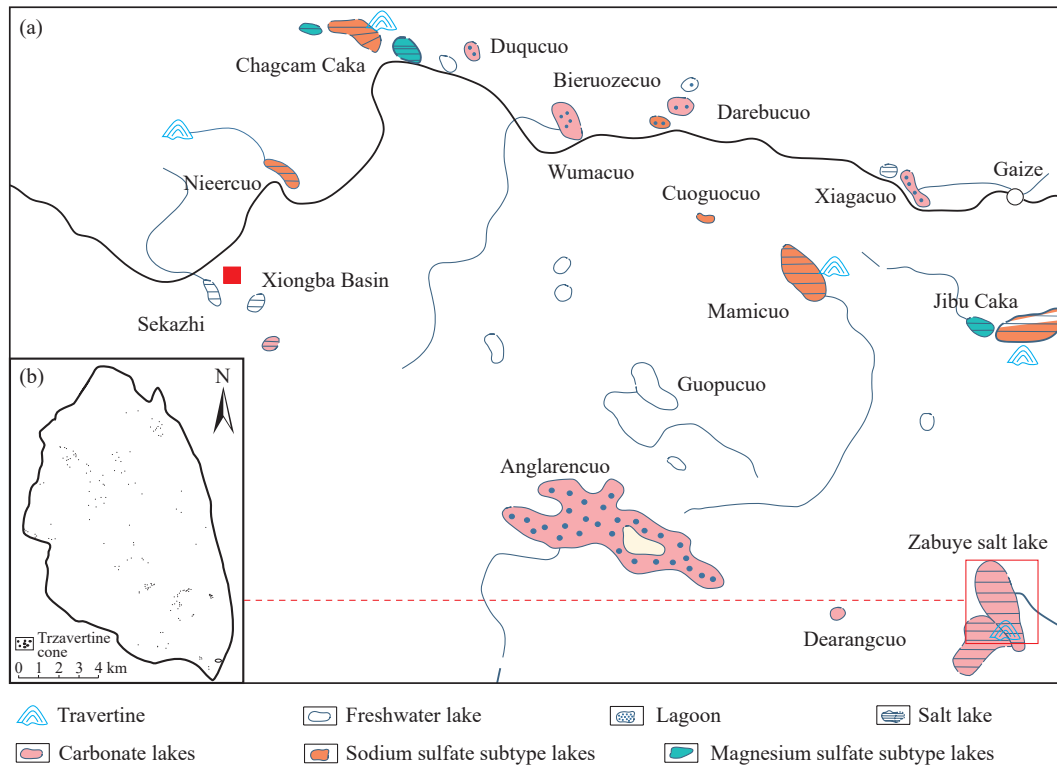


Fig. 4. Map showing the distribution of travertine in the lithium ore concentration area of the Zabuye Salt Lake a– Distribution of travertine cones in the area and different types of salt lakes based on water chemistry; b– Distribution of travertine cones in the Zabuye Salt Lake (Zheng MP et al., 1989b).

hydrothermal activity carried numerous lithium- and boron-containing substances, which were hardly deposited. Until the Last Glacial Maximum (30 ka BP), the big lakes were completely disintegrated. Since the Last Deglaciation (16 ka BP), soluble minerals such as deep lithium (boron) that converged over a prolonged period were suddenly scattered under the action of physicochemical differentiation and the gravitational field, forming many lithium-bearing salt lakes on the plateau (Zheng MP et al., 2006), including over 50 lithium-rich salt lakes (Fig. 8).

The lithium content in seawater (n_1) is $(0.178 \text{ mg/L}) \times 10^3 / \sum \text{salt} = 0.005$, and that in a lithium-bearing salt lake (n_2) ranges from 0.1–10, with n_2/n_1 ratio ($N = n_2/n_1$) between 50–1000.

According to the research on the Zabuye Salt Lake Mining District in Tibet, the supernormal parameter n_2 is 6–8 for superlarge-large lithium-bearing salt lakes and 0.5–5 for ordinary small and medium-sized ones in the area.

As shown by the calculation of the lithium content of partial lithium-bearing salt lakes in the study area, four salt lakes, marked by blue boxes in Fig. 9, are superlarge or medium-sized. They exhibit lithium/salt ratios of above 6, which is 1200 times that of seawater.

With a watershed as a boundary, the Zabuye lake chain is divided into two multi-order lake chains (complex lake chains). As the lake surface elevation decreases northward from the Dehuri Lake—a freshwater lake, the lithium/salt ratio gradually increases until the low-order Laguocuo Salt Lake and Jibu Caka, where large lithium deposits have been

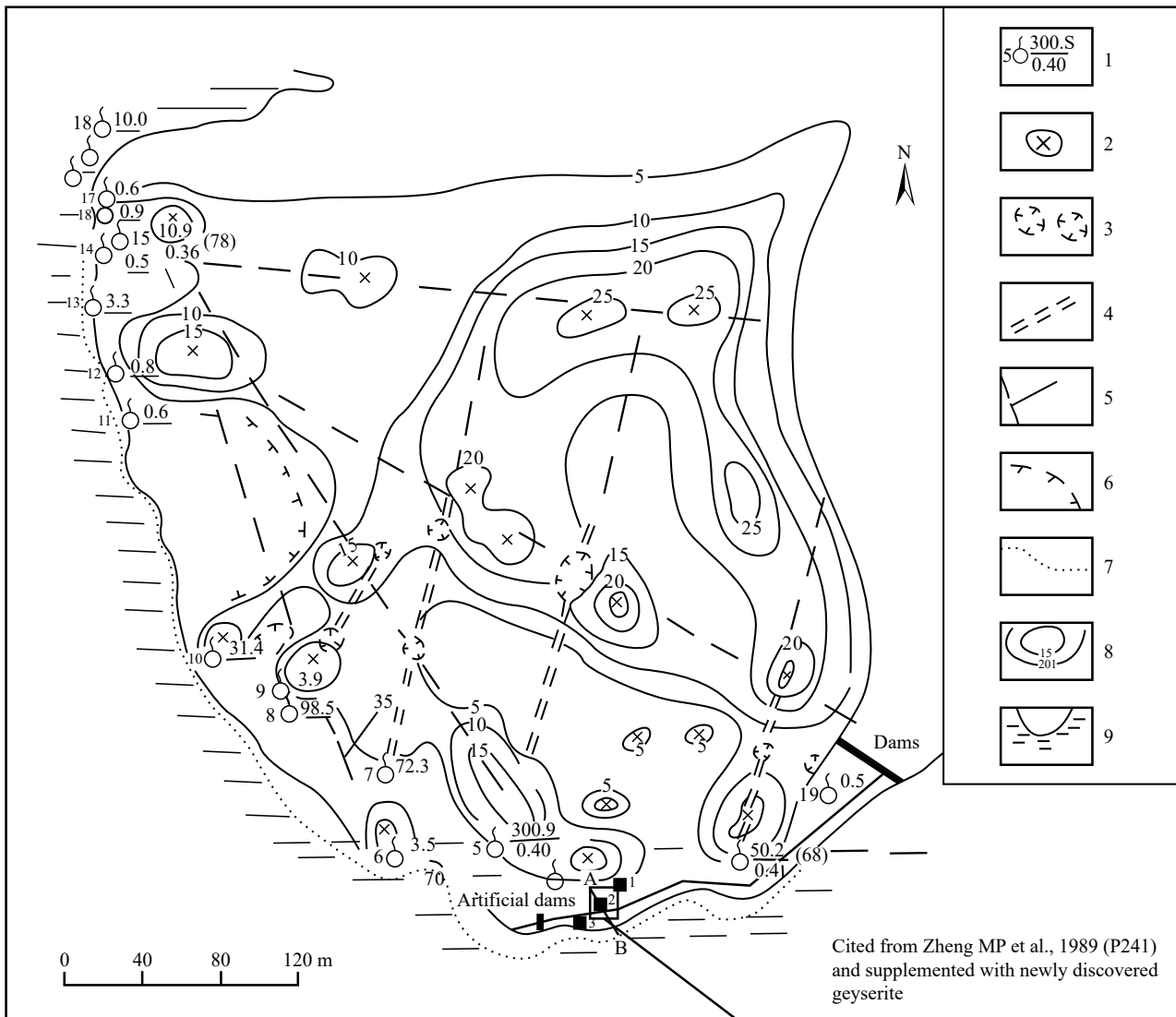
formed. By contrast, the lithium deposits of the north and south lakes of the Zabuye Salt Lake can be found southward from the watershed (Fig. 10).

The latest research shows that the lower-order Mamicuo Salt Lake is also connected to the Laguocuo Salt Lake in the case of a high water level. With a lithium/salt ratio of 6.49, the Mamicuo Salt Lake forms a superlarge lithium deposit.

3.3.2. Metallogenic epochs of lithium-bearing salt lakes in Tibet and their responses to paleoclimatic changes

The chronological study of salt lakes in Tibet shows that the lithium-bearing salt lakes in Tibet exhibit the youngest formation age and metallogenic epochs nationwide. Although lithium is prone to accumulate in water, it accumulates and precipitates only in carbonate-type salt lakes under a dry and warm climate. Therefore, deposited lithium can also reflect the characteristics of paleoclimatic evolution. By contrast, minerals including mirabilite and soda, which were deposited in a cold environment, can reflect cold and arid paleoclimates.

The lithium carbonate in salt lakes on the Tibetan Plateau was significantly deposited at 13–12.7 ka BP (the Bølling), 9.8–9.5 ka BP (the Boreal), and 4.1–4 ka BP, with the last period witnessing a major lithium depositional event (Zheng MP et al., 2007; Zheng MP et al., 2007; Ma ZB et al., 2010; Ling Y et al., 2017). Besides, Europe experienced the warmest climate at 13–12.7 ka BP (the Bølling) (Lowe JJ and Weker MJC, 1984). During the Holocene Megathermal from 6.5–4 ka BP, the temperature in the Northern Hemisphere was 4–5°C higher than the present temperature (Man ZM, 2009).



- 1—spring no., flow rate (l/s)/total salt content/(g/l)
- 2—spring orifice of ancient travertine
- 3—karst lake
- 4—dissolution channel and karst river
- 5—measured and inferred fault
- 6—travertine terrace subjected to lacustrine dissolution
- 7—distribution line of modern travertine
- 8—contour and relative height/m
- 9—lake water

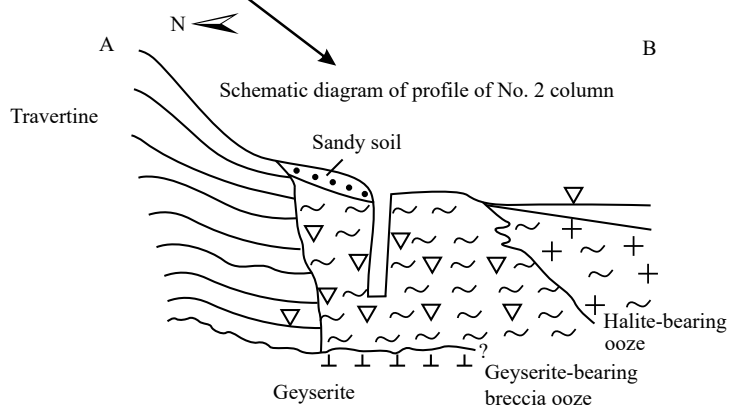


Fig. 5. Map showing the locations of geysersite in the Zabuye travertine island.

As a response, a large quantity of lithium carbonate was deposited on the Tibetan Plateau at the end of the Holocene Megathermal (Fig. 11).

To verify the reliability of the above-mentioned minerals as paleoclimatic indicators, this study conducted field experiments and meteorological temperature observations in a salt pan of the Zabuye Salt Lake (Fig. 12). Based on continuous observations of the salt deposits in the salt pan

from December 1, 2002 to September 24, 2003, it is found that the salt deposits can be divided into three stages (Table 4).

3.3.3. Metallogenic characteristics of lithium in multistage salt lakes in Lithium Triangle, South America

The multi-order lake chains in the Lithium Triangle, South America exhibit consistent lithium accumulation and metallogenic regularities with those in China, both showing

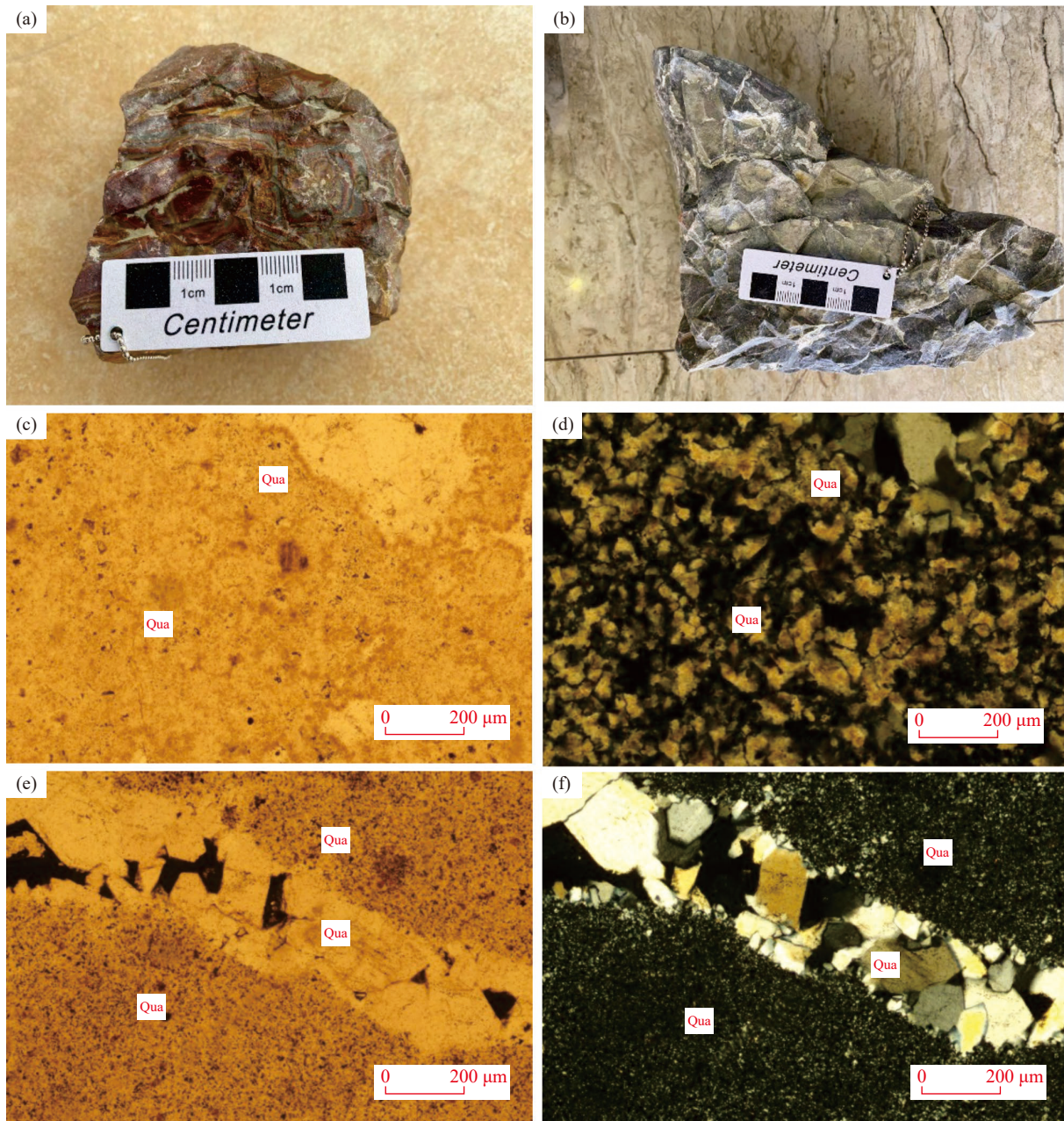


Fig. 6. Hand specimens of the geysers in the Zabuye island and their microscopic mineral structures. a–geysers, annular ripple texture; b–geysers, breccia texture; c–geysers, under single-polarized light; d–geysers, under cross-polarized light; e–Quartz in fissures, under single-polarized light; f–Quartz in fissures, under cross-polarized light.

similar metallogenic epochs (i.e., the Cenozoic, especially the Miocene) and more abundant lithium resources in salt lakes situated in low terraces (Table 5; Fig. 13; Fig. 14).

Salt lakes are found in northern Argentina and a portion of Chile that borders Argentina, such as the Hombre Muerto, Cauchari-Olaroz, and Maricunga salt lakes, which cover areas of around 565 km², over 508 km², and 1045 km², respectively (Table 5). With a comparatively high average elevation, these salt lakes are smaller than those in areas at low elevations. In Chile and central-south Bolivia, where the average altitude is lower, a small number of large-scale salt lakes with considerable resources and prolonged salt-forming periods are distributed, including the Coipasa (elevation: 3656 m), Uyuni (elevation: 3650 m), and Atacama salt lakes (elevation: 2300

m), which cover areas of around 2500 km², 10582 km², and 3200 km², respectively (Table 5). In addition, all these salt lakes have a hydrochemical type of the magnesium sulfate subtype, which is somewhat consistent with the hydrochemical type of the Qaidam Basin.

Overall, as indicated by the comparative analysis of typical lithium-bearing salt lakes at home and abroad, the lithium in salt lakes on plateaus tends to migrate and accumulate toward low-lying areas under the action of gravity field and chemical differentiation. Therefore, the salt lake groups on the planation surface at lower elevations are characterized by long lithium metallogenic periods, a large catchment area, large lithium metallogenic scales, and a small number of salt lakes. By contrast, the salt lake groups on the

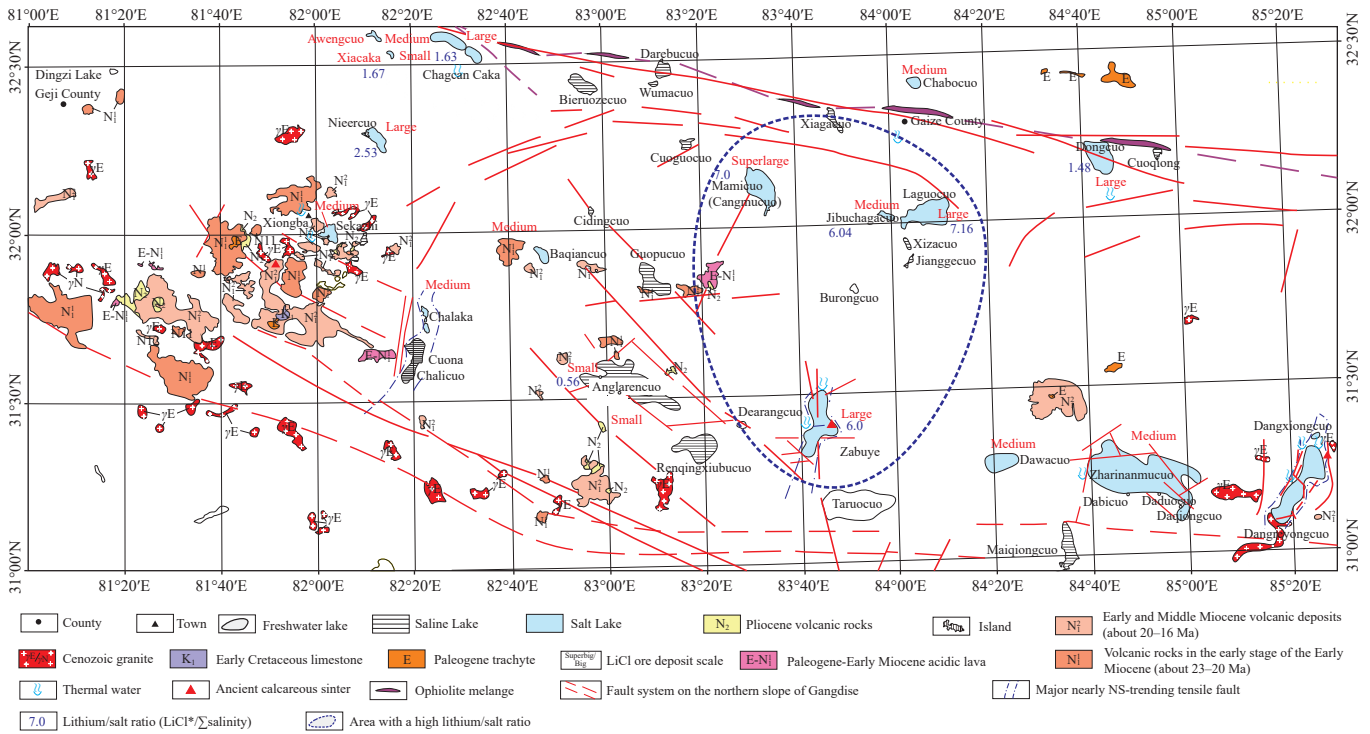


Fig. 9. Map showing the distribution of lithium/salt ratios of the lithium ore concentration area in the Zabuye Salt Lake.

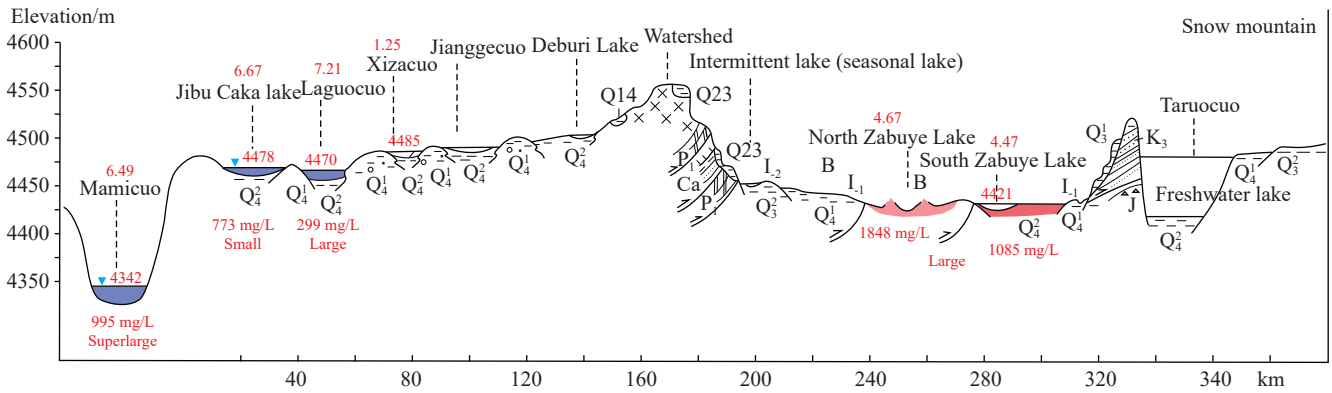


Fig. 10. Enrichment and mineralization mechanisms of the Zabuye lake chain (red numbers denote the lithium/salt ratios of lake water).

DH et al., 2022).

4. Lithium extraction technologies

4.1. Lithium extraction from clay-type lithium deposits

The current methods for lithium production from solid lithium deposits primarily include the processes of acid (Fig. 15), alkaline, salt roasting, and high-temperature chlorination (Kesler SE et al., 2012; Meshram N et al., 2014; Choubey PK et al., 2016; Swain B, 2016). Despite a high recovery rate, the acid process suffers many disadvantages, such as complicated technological processes, high costs, high content of impurities, difficulty in removing impurities, easy entrainment of lithium by mixed salts, and the emission of waste gas and numerous waste residues that cause environmental pollution (Xiao MS et al., 1997; Koltsov V et al., 2016). In contrast, the alkaline process is environment-friendly and features high

selectivity and simple technological processes. However, this process has the disadvantages of a low recovery rate and high cost (Deng FY et al., 1999). The high-temperature chlorination process, with Cl₂ as the chlorinating agent, exhibits a high recovery rate and fewer wastes in extracting alkaline metals (e.g., lithium) from ores. However, this process requires high anti-corrosion performance of the whole set of process equipment and complicated technological processes (Barbosa TR et al., 2013; Barbosa LI et al., 2014). To reduce the use of acids and alkalis, the costs, and equipment maintenance workload, some researchers have proposed salt roasting processes, which can be predominantly divided into roasting with sulfate and chloride salts. The principle of sulfate roasting process is shown in Equation 4.1. In this process, sulfate salts are first converted into soluble lithium salts through high-temperature crystal transformation. Then, the soluble lithium salts are precipitated and separated to yield lithium products. However, since potassium salts are

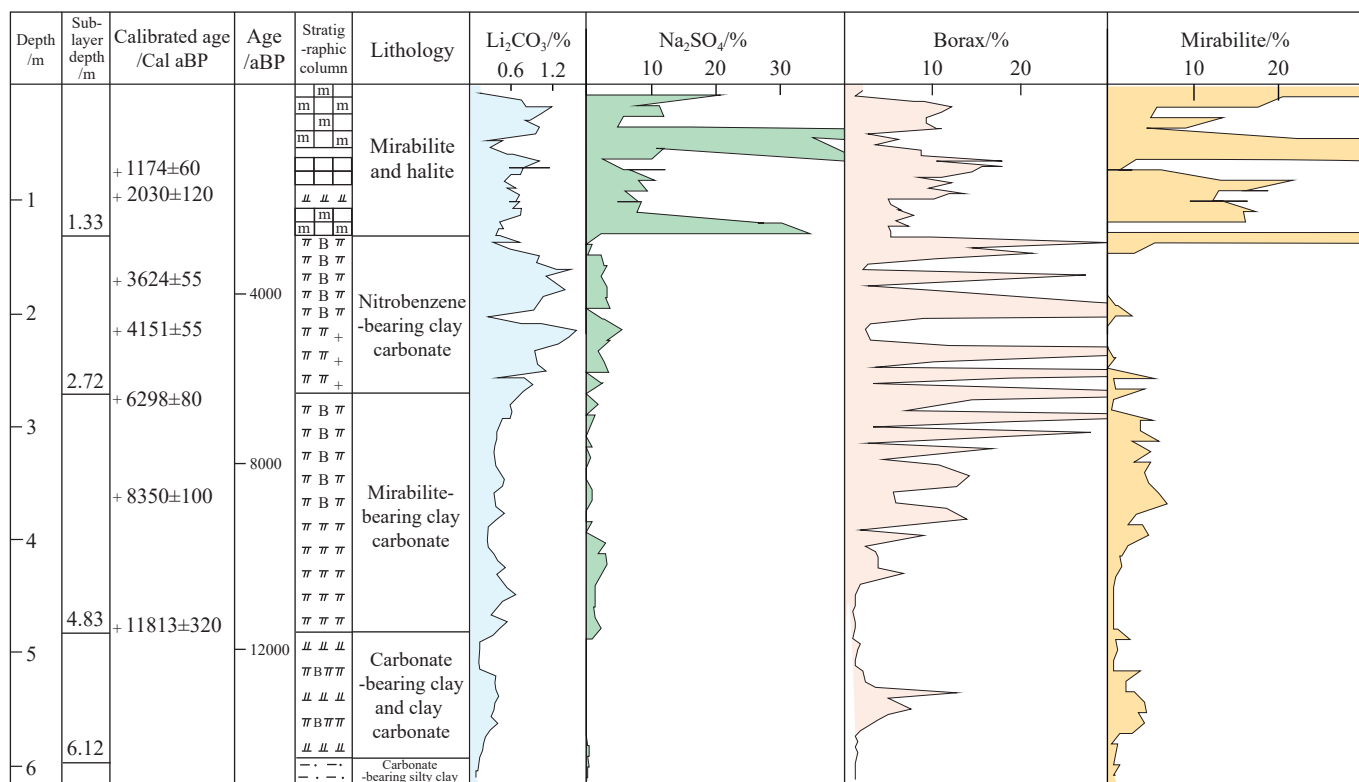


Fig. 11. Paleoclimatic records since 128 Ka obtained from borehole SZK02 in the Zabuye Salt Lake, Tibet (after Zheng MP et al., 2007; Zheng et al., 2007; Ma ZB et al., 2010; Ling Y et al., 2017).

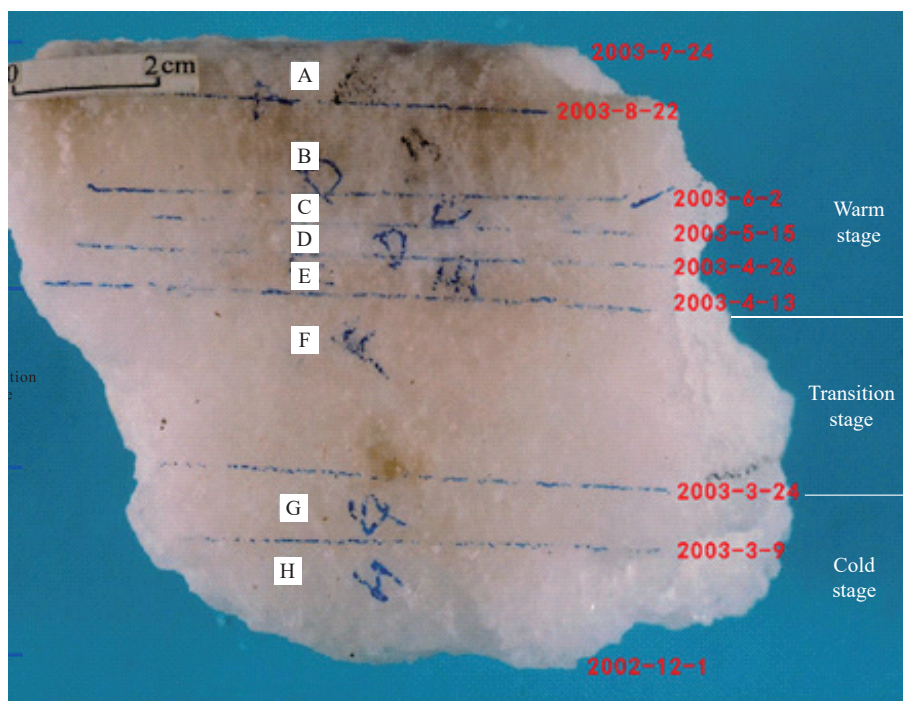


Fig. 12. Salt deposits in the salt pan of the Zabuye Salt Lake.

also strategic resources, the further recovery of lithium from potassium salts yielded from the process will further increase the costs. Therefore, it is necessary to further improve the process (Arne SK and Johan WS, 1941). The roasting with chloride salts serves as a research hotspot currently, with the fundamental principle shown in Equation 4.2. This process

enjoys a conversion rate of high lithium salts. However, the waste residue treatment in this process is challenging (Barbosa LI et al., 2015).

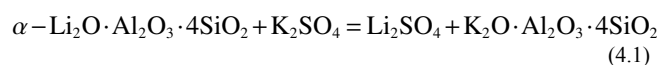
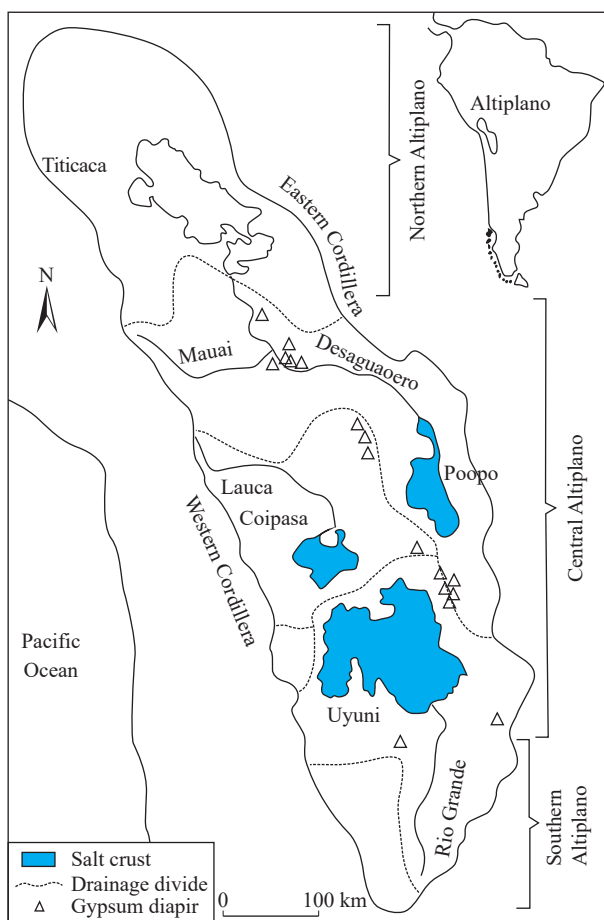


Table 4. Results of field experiments and meteorological temperature observations in the Zabuye Salt Lake.

Time span	Climate	Average temperature/°C	Typical minerals
December 1, 2002 to March 24, 2003	Cold stage	−4.8	Mirabilite (natron)
March 25, 2003 to April 13, 2003	Transitional stage	−1.4	Mirabilite (thenardite), a small amount of Li ₂ CO ₃
April 14, 2003 to September 24, 2003	Warm stage	9.8	Li ₂ CO ₃ , thenardite, trona

Table 5. Resources and distribution of major lithium-bearing salt lakes in South America's Lithium Triangle.

Serial number	Salt lake	Water surface elevation/m	Area/km ²	Lithium content/(mg/L)	Resources/Reserves/million tons	Country
1	Atacama Salt Lake	2300	3200	1500	6.3	Chile
2	Uyuni Salt Lake	3650	10582	530	10.2	Bolivia
3	Coipasa Salt Lake	3656	2500	483	15	Bolivia
4	Maricunga Salt Lake	3750	1045	1020	1.5	Chile
5	Cauchari-Olaroz Salt Lake	3900	508	690	6.4	Argentina
6	Hombre Muerto Salt Lake	4300	565	744	7.8	Argentina

**Fig. 13.** Resources and distribution of major lithium-bearing salt lakes in South America's Lithium Triangle.

The occurrence state of lithium in clay-type lithium deposits determines the selection of metallurgical techniques. The leaching process is mostly employed to extract lithium from adsorbent clay minerals, while the combination of the roasting and acid processes is primarily used to extract lithium from lattice displacement lithium containing minerals (Ren FT and Zhang J, 2013). The selection of metallurgical techniques is detailed in Fig. 16.

4.2. Salinity gradient solar pond (SGSP) method

The primary methods for extracting lithium from salt lakes include the SGSP, membrane, adsorption, and extraction methods (Zheng MP et al., 2006; Xu S et al. 2021). Among them, the SGSP method has played a significant role in Tibet with limited energy supply. Developing and utilizing solar pond technology based on local conditions contribute to the formation of environment-friendly industries, such as power generation, chemical production of salt pans, heating, planting combined with breeding, and livestock product processing. This can counteract the poor transportation and energy conditions in western China. Therefore, the solar pond technology has great potential for development.

Based on the salinology theory and following the guiding ideology of “working hard, adapting to local conditions, utilizing local resources, and fostering strengths while circumventing weaknesses”, the authors of this study determined a process technology route for the exploitation and production of liquid lithium deposits in the Zabuye Salt Lake by skillfully utilizing solar and cold resources given the insufficient mineral resources, alpine and anoxic environment, and inconvenient transportation conditions in Tibet. This process technology, incorporating the SGSP method with independent intellectual property rights and the new brine production process by freezing (Fig. 17), has won the excellence award of the China Patent Award (Fig. 18). Through years of field experiments from small to large scales and then to process experiments, the first author of this study achieved the industrialization of this process technology in 2006 and has constantly provided relevant technical support (Fig. 19).

Raw brine (Table 6) is first pumped from the salt lake into the pre-sun-drying pond, where the brine depth is generally maintained at 0.6–0.8 m. The purpose is to achieve preliminary brine concentration and the precipitation of a large quantity of NaCl. After the initial brine concentration, the lithium-ion concentration in the pre-sun-drying pond can increase from 0.8–1.2 g/L to 1.0–1.4 g/L. Then, the brine flows to the second-order evaporation pond by gravity, where the brine depth is generally kept at 0.4–0.6 m, and the lithium-

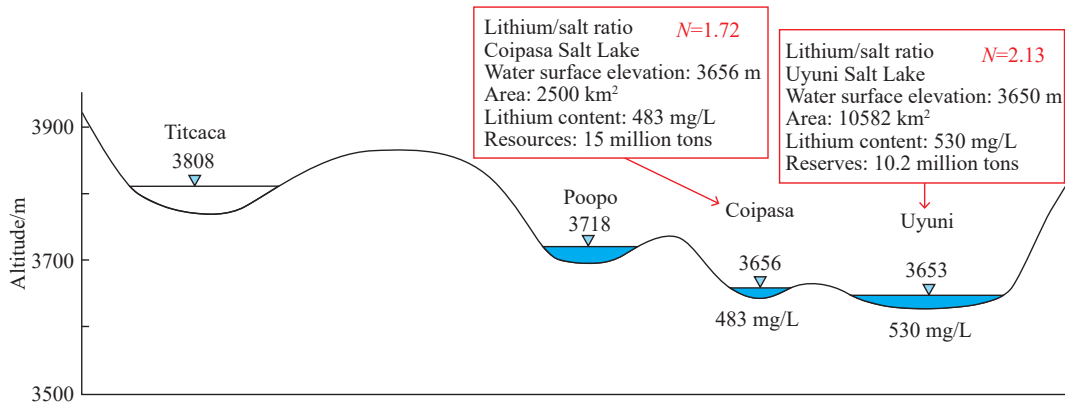


Fig. 14. Schematic diagram showing the multistage mineralization of lithium-bearing salt lakes in South America.

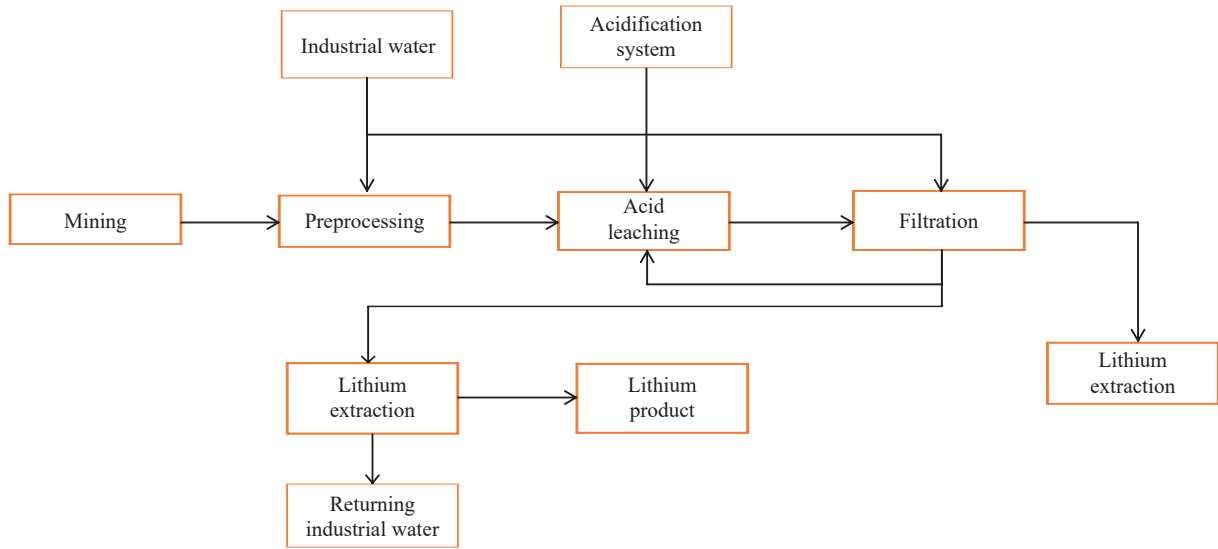


Fig. 15. Flowchart showing lithium extraction using the acid process.

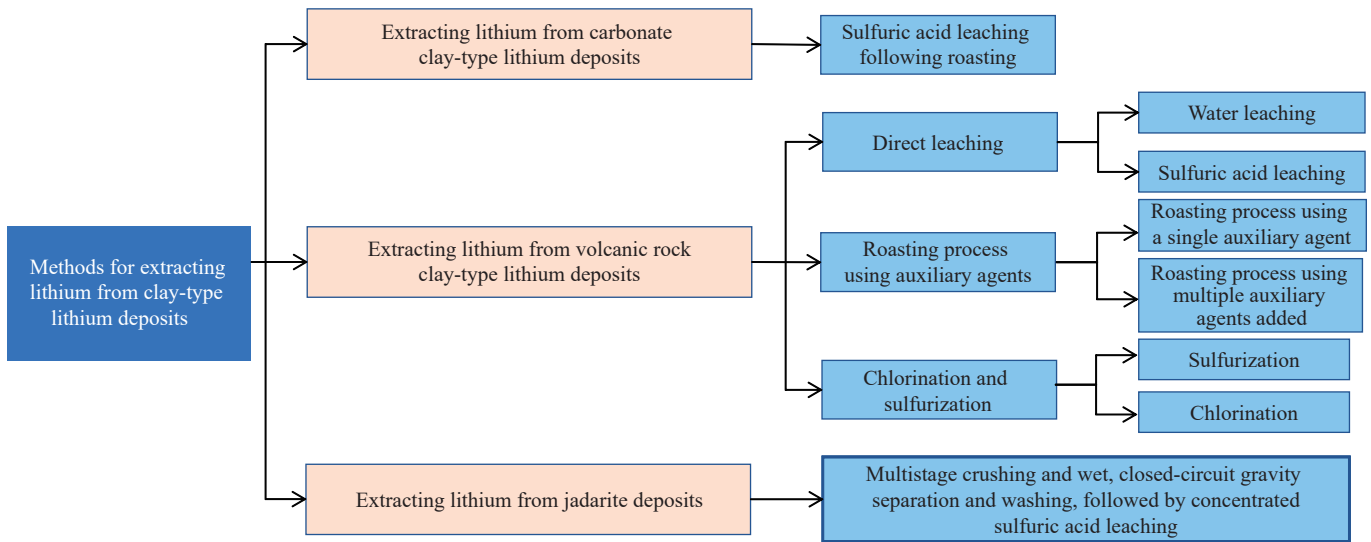


Fig. 16. Processes for extracting lithium from clay-type lithium deposits.

ion concentration rises to 1.2–1.6 g/L. The lithium-ion concentration of brine in this pond must be strictly controlled. Subsequently, the brine is concentrated in the third-order evaporation pond until lithium carbonate is almost saturated.

In this pond, the lithium-ion and carbonate concentrations generally increase to 2.0–2.2 g/L and 25–28 g/L, respectively in winter and 1.4–1.6 g/L and 40–45 g/L, respectively in summer. The third-order evaporation pond is composed of

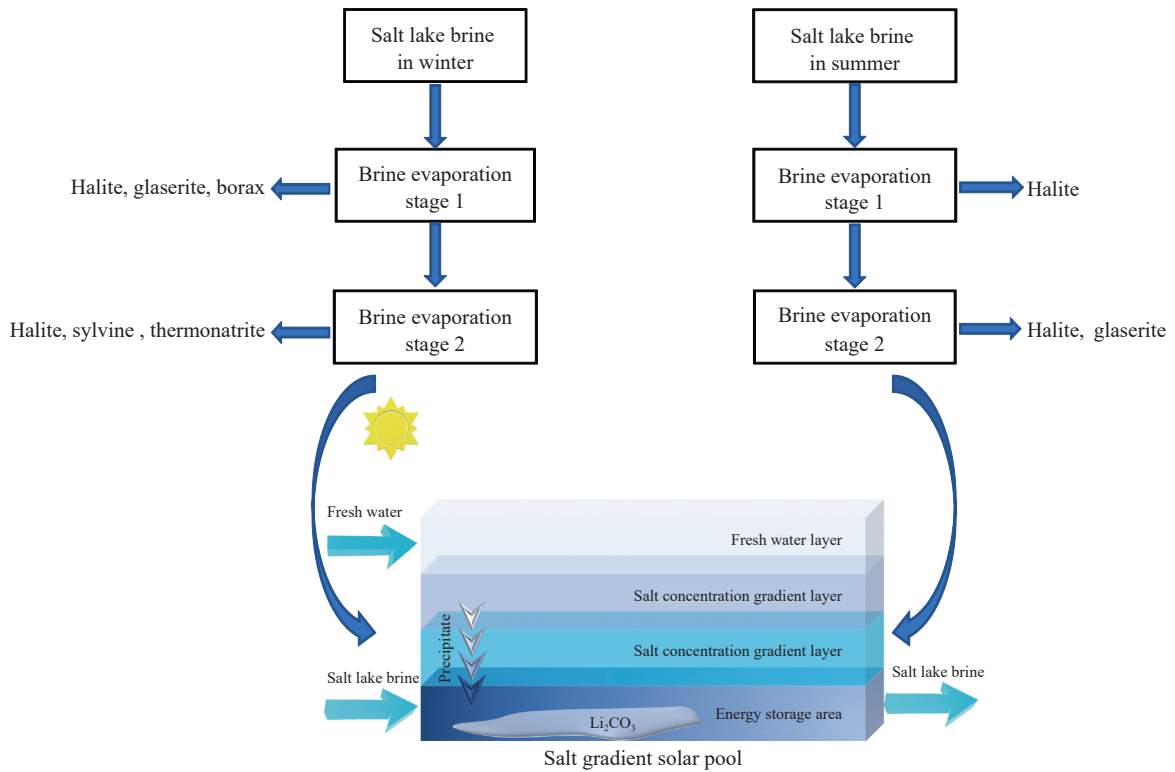


Fig. 17. Flow chart showing the lithium extraction using the SGSP process (Ding T et al., 2022).



Fig. 18. Patent certificate for the SGSP process and the excellence award certificate of the China Patent Award for the technology.

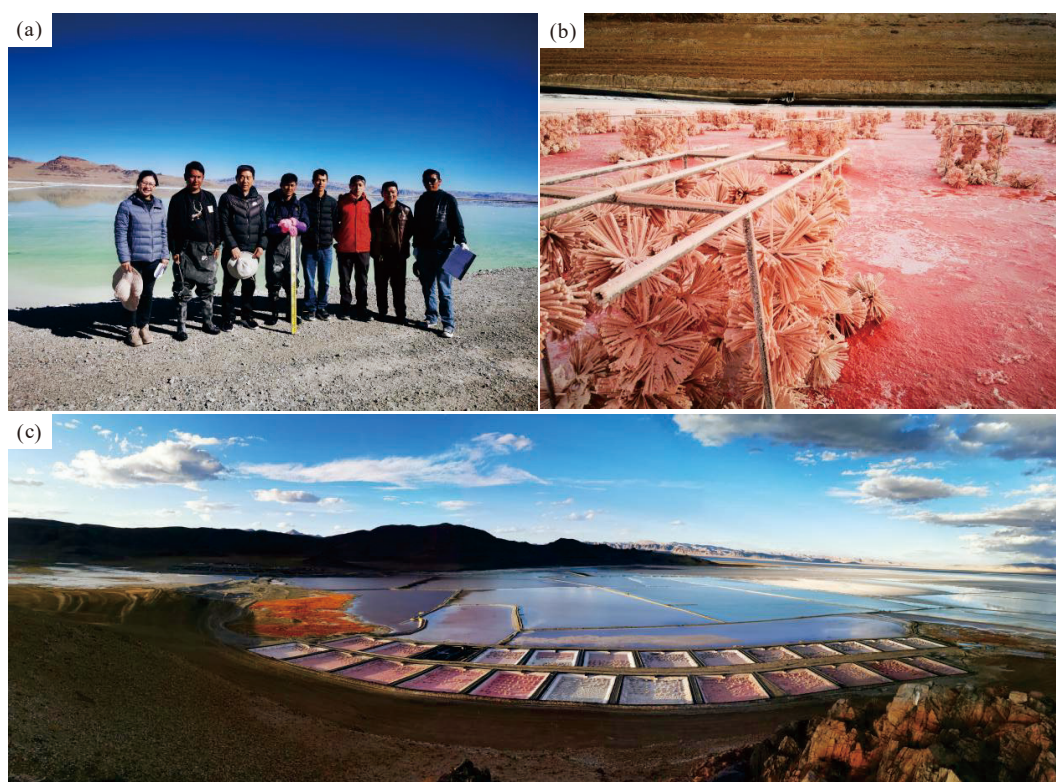


Fig. 19. Industrialization of lithium extraction in the Zabuye Salt Lake, Tibet. a—photo showing Bu LZ and his team working in the Zabuye Salt Lake; b—an improved technique for enhancing the recovery rate of lithium carbonate through stereocrystallization—the crystallization effect of lithium carbonate mixed salts on the nucleation substrate after brine discharge from the solar pond; c—a scene of the Zabuye Salt Lake (taken in 2022).

Table 6. Chemical composition of raw brine in the Zabuye Salt Lake.

Ion	Li ⁺	K ⁺	Na ⁺	Mg ²⁺	Ca ²⁺	Rb ⁺ (mg/L)	Cs ⁺ (mg/L)	Br ⁻ (mg/L)	Cl ⁻	SO ₄ ²⁻	B ₂ O ₃
(g/L)	0.92	23.28	129.64	/	/	37	12.5	337	157.81	15.25	5.20

several small ponds, which can be flexibly combined in series or parallel for brine production depending on seasons and the crystallization pond's demand for brine. The brine with almost saturated lithium carbonate either flows by gravity or is pumped into the brine storage pond for future use. To prevent large quantities of lithium carbonate from precipitating due to temperature fluctuations, a deep brine depth of approximately 0.6 m is usually maintained in the third-order evaporation pond in order to achieve a stable brine temperature. The brine in the brine storage pond is injected into the crystallization pond (the solar pond), which absorbs and stores solar radiation energy to increase the temperature of the saturated lithium carbonate solution in the crystallization pond. As a result, the lithium carbonate is oversaturated, crystallizes, and precipitates. The brine in the crystallization pond is generally kept at a depth of 2–2.5 m, and its temperature can rise to 30°C–40°C over about a month and a half or two months in spring and to 45°C after about a month in summer. Following the precipitation of lithium carbonate, the mother liquid (tail brine) flows into the tail brine pond. The tail brine will either be used to supplement the brine in the evaporation ponds or be directly injected into the solar pond after re-sun-drying in the tail brine pond, depending on the actual need. The entire evaporation and

crystallization process relies on solar energy alone and thus is safe, harmless, and cost-effective. Without any chemical reagents being added throughout the process, concentrates with lithium carbonate grades of 75% or higher (composition: 75% Li₂CO₃, 8%–10% NaCl, 2%–5% KCl, and 7%–10% Na₃Mg (CO₃)₂Cl) can be obtained directly. The closed cycle of raw brine allows brine resources to be fully utilized. Furthermore, the process is simple, environmentally friendly, and totally green and clean. The solar pond consists of the upper convective zone, the middle non-convective zone (also known as the salinity gradient zone), and the lower convective zone. The upper convective zone, usually composed of freshwater, is primarily used to maintain the salinity gradient of brine in the pond and resist wind disturbance. The middle non-convective zone, with salinity and temperature gradients from top to bottom, functions as a thermal insulation layer of the solar pond. The lower convective zone, composed of high-concentration salt solution, plays a significant role in collecting and storing solar energy.

When solar radiation energy reaches the water surface, it is absorbed, reflected, and refracted into the water. The solar radiation energy refracted into the water is absorbed by the water zone by zone. The remaining part reaches and is absorbed by the pond bottom, thus heating up the bottom. If

the pond walls and bottom are constructed using thermal insulation materials and the area of the pond bottom is much larger than that of the pond wall, little heat will dissipate from the pond walls and bottom. As a result, the solar radiation energy absorbed by the pond bottom will be mostly transferred to water, thus increasing the water temperature of the lower convective zone. Normally, with an increase in the water temperature of the lower convective zone, thermal convection will occur naturally to balance the overall water temperature of the pond. However, the presence of the salinity gradient in the solar pond prevents the occurrence of thermal convection. In other words, the density difference formed by the salinity gradient in the solar pond is sufficient to suppress the density difference caused by the temperature gradient, thus inhibiting thermal convection. Consequently, the water temperature of the lower convective zone gradually increases, forming a temperature gradient from top to bottom and maintaining its thermal stability. In this case, the heat in the lower convective zone can only be transferred upwards to the surface water through thermal conduction, while the thick (usually 1–1.5 m) non-convective zone exhibits a high insulation performance. Water has a rather high thermal resistance (thermal conductivity: $0.654 \text{ W/m}^2 \cdot ^\circ\text{C}$ at 60°C), and the insulation effect of a 1-m-thick water zone is comparable to that of asbestos with a thickness of over 10 cm. Therefore, the lower convective zone of the solar pond works as a closed system. As the solar radiation energy continuously reaches the pond bottom, where almost no thermal energy dissipates, the water temperature of the lower convective zone continues to rise and is maintained at a high level, which will cause lithium carbonate to precipitate from the salt lake.

At present, the authors' team is updating the solar pond technology and developing the technological upgrading route, such as pond wall insulation, adsorption technology coupling in mimetic mineralogy, and solar energy-based crystallization acceleration, aiming to enhance the applicability and crystallization yield of solar ponds. Given the considerable quantities of lithium-bearing clay minerals at the bottom of the Zabuye Salt Lake, the authors' team has explored a preliminarily feasible process route by coupling the SGSP technique with the lithium extraction process from lithium-bearing clay minerals.

4.3. Lithium extraction from lithium from hard rocks

At present, China's lithium production still focuses on lithium extraction from hard-rock lithium deposits, which suffers shortcomings related to resources, environment, and economy compared to lithium extraction from brine. Gao *et al.* (2023) introduced the research progress in lithium extraction from spodumenes, lepidolites, petalites, and zinnwaldites using the processes of acid, alkaline, salt roasting, and chlorination. They analyzed the resource intensity, environmental impact, and costs of industrial lithium extraction from spodumenes and lepidolites. Research shows that the sulfuric acid process, despite a high lithium recovery rate, requires complicated processes and high energy consumption. The alkaline and chlorination processes allow direct reaction with lithium ores, thus reducing energy

consumption. However, it is necessary to optimize the reaction conditions to ensure the safety of equipment and operations. The salt roasting process requires a high material flux and high energy consumption, necessitating adjusting the sulfate proportion to enhance the lithium recovery rate and reduce production costs. Compared to lithium extraction from brine, extracting lithium from ores consumes more resources and energy, making it less competitive. Therefore, in addition to enhancing the lithium recovery rate and reducing energy consumption, the processes for lithium extraction from hard-rock ores should also focus on comprehensive utilization and cost reduction.

5. Conclusions

(i) The lithium resources in the world can be divided into 10 types. The proportions of various lithium deposits exploited are significantly influenced by the market-oriented economy. As indicated by historical experience, lithium resources are primarily exploited from salt-lake lithium deposits in the case of a low lithium price, while a high lithium price can drive the rapid development of other types of lithium deposits such as the hard rock type. Over recent years, the extensive utilization of lithium as a new energy has promoted the prospecting and exploitation boom of lithium deposits, objectively promoting the investigation and research of lithium resources. Currently, the lithium price has sharply decreased after a surge. In the long run, only a reasonable lithium price is beneficial for the steady development of the lithium industry.

(ii) As revealed by research on the origin of Cenozoic exogenetic lithium deposits, the materials in the lithium deposits primarily originate from the lithium-bearing anatectic magmas in the deep oceanic crust, demonstrating specific metallogenic epochs and exclusive magmas. The lithium deposits of the salt lake, geothermal, and volcanic deposit types are intimately linked to lithium-bearing tuffs and geothermal water, which, coupled with arid, cold, and warm climates, contribute to lithium mineralization. These deposits tend to migrate and accumulate toward low-lying areas and display supernormal enrichment. Comparison between the present and past can also provide a reference for analyzing the origin and mineralization of Paleozoic lithium deposits. Presently, it is necessary to further ascertain the occurrence states and material sources of lithium in Neopaleozoic silico-aluminous clay-subtype lithium deposits in China, as well as the material source of lithium in deep brine in the country.

(iii) For multi-sphere discussion from the perspective of the earth science system, besides the lithosphere and hydrosphere, the interactions of both spheres with the atmosphere should also be considered. Furthermore, it is necessary to investigate the mineralization of exogenetic lithium deposits by combining tectono-geochemistry, paleoatmospheric circulation, and salinology studies.

(iv) The authors' team has developed an innovative technology for direct lithium extraction from salt lakes without adding any reagents, which is unprecedented. This technology is cost-effective, with a direct cost of only 9000 yuan/t and a total cost of 20000 yuan/t (according to appraisal

and the Bu LZ's work group has improved the lithium recovery rate using the technique of stereocrystallization, and the total cost is still maintained at the level of 20000 yuan/t, by China International Engineering Consulting Corporation), having yielded satisfactory economic benefits. From a developmental perspective, only mature, cost-effective, and environment friendly lithium extraction technologies can serve as a foundation for the sound development of the lithium industry.

CRedit authorship contribution statement

Mian-ping Zheng, En-yuan Xing, Xue-fei Zhang, Ming-ming Li, Ling-zhong Bu and Chuan-yong Ye prepared the manuscript. Dong Che, Jia-huan Han drew all the figures. Mian-ping Zheng supervised the findings of this work. All authors discussed the results and contributed to the final manuscript.

Declaration of competing interest

The authors declare no conflicts of interest.

Acknowledgement

This work was funded by the major research program of the of National Natural Science Foundation of China entitled *Metallogenic Mechanisms and Regularity of the Lithium Ore Concentration Area in the Zabuye Salt Lake, Tibet* (91962219), Science and Technology Major Project of the Tibet Autonomous Region's Science and Technology Plan (XZ202201ZD0004G01) and a geological survey project of China Geological Survey (DD20230037). The authors would like to extend our gratitude to reviewers of this manuscript for their valuable comments. Our thanks also go to colleagues Qian Wu, Tao Ding and Jin-xin Jian for their assistance to this study.

References

- AGU Fall Meeting 2018. V14B: Lithium Resources in Continental Brines, Pegmatites, and Lacustrine Sediments. <https://agu.confex.com/agu/fm18/meetingapp.cgi/Session/51511>.
- Arne SK, Johan WS. 1941. Method of recovering lithium salts from lithium-containing minerals: US24041638A. 1941-01-28.
- Barbosa LI, González JA, Ruiz MDC. 2015. Extraction of lithium from β -spodumene using chlorination roasting with calcium chloride. *Thermochimica Acta*, 605, 63–67. doi: [10.1016/j.tca.2015.02.009](https://doi.org/10.1016/j.tca.2015.02.009).
- Barbosa LI, Valente G, Orosco RP. 2014. Lithium extraction from beta-spodumene through chlorination with chlorine gas. *Minerals Engineering*, 56, 29–34. doi: [10.1016/j.mineng.2013.10.026](https://doi.org/10.1016/j.mineng.2013.10.026).
- Barbosa LI, Valente NG, González JA. 2013. Kinetic study on the chlorination of β -spodumene for lithium extraction with Cl_2 gas. *Thermochimica Acta*, 557, 61–67. doi: [10.1016/j.tca.2013.01.033](https://doi.org/10.1016/j.tca.2013.01.033).
- Benson TR, Coble MA, Dilles JH. 2023. Hydrothermal enrichment of lithium in intracaldera illite-bearing claystones. *Science Advances*, 9(35), eadh8183. doi: [10.1126/sciadv.adh8183](https://doi.org/10.1126/sciadv.adh8183).
- Benson TR, Coble MA, Rytuba JJ, Gail AM. 2017. Lithium enrichment in intracontinental rhyolite magmas leads to Li deposits in caldera basins. *Nature Communications*, 8(1), 270. doi: [10.1038/s41467-017-00234-y](https://doi.org/10.1038/s41467-017-00234-y).
- Bradley DC, McCauley AD, Stillings LL. 2017. Mineral-deposit model for lithium cesium tantalum pegmatites: U. S. Geological Survey Scientific Investigations Report 2010-5070-O, 1–48. doi: [10.3133/SIR20105070O](https://doi.org/10.3133/SIR20105070O).
- Bradley DC, Stillings LL, Jaskula BW, Munk, LA, McCauley AD. 2017. Lithium, chap. K. In: Schulz KJ, DeYoung JH, Seal RR, Bradley DC (eds.), *Critical mineral resources of the United States-Economic and environmental geology and prospects for future supply*: U. S. Geological Survey Professional Paper 1802, K1–K21. doi: [10.3133/pp1802K](https://doi.org/10.3133/pp1802K).
- Chen P and Chai DH. 1997. *Sedimentary Geochemistry of Carboniferous Bauxite Deposit in Shanxi*. Taiyuan: Shanxi Science and Technology Press, 1–194 (In Chinese with English Abstract).
- Choubey PK, Kim MS, Srivastava RR, Lee JC. 2016. Advance review on the exploitation of the prominent energy-storage element: lithium (I): From mineral and brine resources. *Minerals Engineering*, 89, 119–137. doi: [10.1016/j.mineng.2016.01.010](https://doi.org/10.1016/j.mineng.2016.01.010).
- Christmann P, Gloaguen E, Labbé JF, Melleton J, Piantone P. 2015. Chapter 1-Global Lithium Resources and Sustainability Issues. In: Chagnes A., Światowska J (eds.), *Lithium Process Chemistry*. Elsevier, Amsterdam, 1–40. doi: [10.1016/B978-0-12-801417-2.00001-3](https://doi.org/10.1016/B978-0-12-801417-2.00001-3).
- Davis JR, Vine JD. 1979. Stratigraphic and Tectonic Setting of the Lithium Brine Field, Clayton Valley, Nevada. *Rocky Mountain Association of Geologists*, 421–432.
- Deng FY, Yin TX, Gan WW, He XY. 1999. Comprehensive utilization of potassium, rubidium, and cesium in mother liquor after extracting lithium from lepidolite. *Mining and Metallurgy Engineering*, 19(1), 50–52 (in Chinese with English abstract).
- Ding T, Zheng MP, Peng SP, Lin YH, Zhang XF, Li MM. 2023. Lithium extraction from salt lakes with different hydrochemical types in the Tibet Plateau. *Geoscience Frontiers* 14, 101485. doi: [10.1016/j.gsf.2022.101485](https://doi.org/10.1016/j.gsf.2022.101485).
- Ferrell JE. 1985. Lithium. Chapter in *Minerals Facts and Problems*. United States Bureau of Mine Bulletin 675, 461–470.
- Gao TM, Fan N, Chen W, Dai T. 2023. Lithium extraction from hard rock lithium ores (spodumene, lepidolite, zinnwaldite, petalite): Technology, resources, environment and cost. *China Geology*, 6, 137–153. doi: [10.31035/cg2022088](https://doi.org/10.31035/cg2022088).
- Garrett DE. 2004. *Handbook of Lithium and Natural Calcium Chloride*. Oxford: Academic Press, 1–476.
- Gruber PW, Medina PA, Keoleian GA. 2011. Global lithium availability: A constraint for electric vehicles? *Journal of Industrial Ecology*, 15(5), 760–775.
- Kesler SE, Gruber PW, Medina PA. 2012. Global lithium resources: relative importance of pegmatite, brine and other deposits. *Ore Geology Reviews*, 48(5), 55–69. doi: [10.1016/j.oregeorev.2012.05.006](https://doi.org/10.1016/j.oregeorev.2012.05.006).
- Koltsov V, Novikov PY, Sarychev GA, Tananaev IG. 2016. Experimental investigations during the technology development of sulfuric acid processing of spodumene concentrate. *Tsvetnye Metally*, (4), 18–22. doi: [10.17580/tsm.2016.04.03](https://doi.org/10.17580/tsm.2016.04.03).
- Kunasz IA. 1974. Lithium occurrence in the brines of Clayton Valley Esmeralda County, Nevada. In: Coogan AH (eds). *Fourth International Symposium on Salt*, Houston, 57–66.
- Li BY, Jiang DW, Fu X, Wang L, Gao SQ, Fan ZY, Wang KX, Hugu JLT. 2018. Geological characteristics and prospecting significance of Weilasituo li polymetallic deposit, Inner Mongolia. *Mineral Explorator*, 9(06), 1185–1191 (in Chinese with English abstract). doi: [10.3969/j.issn.1674-7801.2018.06.021](https://doi.org/10.3969/j.issn.1674-7801.2018.06.021).
- Li JK, Liu XF, Wang DH. 2014. The Metallogenetic Regularity of Lithium Deposit in China. *Acta Geologica Sinica*, 88(12), 2269–2283 (in Chinese with English abstract).
- Ling Y, Zheng MP, Sun Q, Dai XQ. 2017. Last deglacial climatic variability in Tibetan Plateau as inferred from n-alkanes in a sediment core from Lake Zabuye. *Quaternary International*, 15–24. doi: [10.1016/j.quaint.2017.08.030](https://doi.org/10.1016/j.quaint.2017.08.030).
- Liu LJ, Wang DH, Liu XF, Li JK, Dai HZ, Yan WD. 2017. The main types, distribution features and present situation of exploration and development for domestic and foreign lithium mine. *Geology in*

- China, 44(2), 263–278 (in Chinese with English abstract). doi: [10.12029/gc20170204](https://doi.org/10.12029/gc20170204).
- Lowe JJ, Walker MJC. 1984. Reconstructing quaternary environments. London: Longman, 1–404.
- Ma ZB, Ma NN, Zhang XF, Wang Y. 2010. $^{230}\text{Th}/^{238}\text{U}$ Chronology of Late Pleistocene Lacustrine Deposits in Zabuye Salt Lake, Tibet. *Acta Geologica Sinica*, 84(11), 1641–1651 (in Chinese with English abstract). doi: [10.19762/j.cnki.dizhixuebao.2010.11.010](https://doi.org/10.19762/j.cnki.dizhixuebao.2010.11.010).
- Man ZM. 2009. Research on Climate Change during the Historical Period of China, Jinan: Shandong Education Press, 1–504 (in Chinese).
- Mcquarrie N, Horton BK, Zandt G. 2005. Lithospheric evolution of the Andean fold-thrust belt, Bolivia, and the origin of the central Andean plateau. *Tectonophysics*, 399(1–4), 15–37. doi: [10.1016/j.tecto.2004.12.013](https://doi.org/10.1016/j.tecto.2004.12.013).
- Meshram P, Pandey BD, Mankhand TR. 2014. Extraction of lithium from primary and secondary sources by pre-treatment, leaching and separation: a comprehensive review. *Hydrometallurgy*, 150, 192–208. doi: [10.1016/j.hydromet.2014.10.012](https://doi.org/10.1016/j.hydromet.2014.10.012).
- O3OJI A A. 1987. Sedimentary and volcanic sedimentary boron deposits. Beijing: Geological Publishing House, 1–222 (in Chinese, Qin GX and Liu JC translated).
- Ren FT, Zhang J. 2013. Chemical separation and enrichment of lithium in aluminous rock in central Guizhou. *Inorganic Chemicals Industry*, 45(3), 19–21 (in Chinese with English abstract). doi: [10.3969/j.issn.1006-4990.2013.03.006](https://doi.org/10.3969/j.issn.1006-4990.2013.03.006).
- Sarchi C, Lucassen F, Meixner A, Caffè PJ, Becchio R, Kasemann SA. 2023. Lithium enrichment in the Salar de Diablillos, Argentina, and the influence of Cenozoic volcanism in a basin dominated by Paleozoic basement. *Miner Deposita*, 58, 1351–1370. doi: [10.1007/s00126-023-01181-z](https://doi.org/10.1007/s00126-023-01181-z).
- Shu LS, Zhu WB, Xu ZQ. 2021. Geological settings and metallogenic conditions of the granite-type lithium ore deposits in South China. *Acta Geologica Sinica*, 95(10), 3099–3114 (in Chinese with English abstract). doi: [10.19762/j.cnki.dizhixuebao.20211152](https://doi.org/10.19762/j.cnki.dizhixuebao.20211152).
- Stanley CJ, Jones GC, Rumsey MS. 2007. Jadarite, $\text{LiNaSi}_3\text{O}_7(\text{OH})$, a new mineral species from the Jadar Basin, Serbia. *European Journal of Mineralogy*, 19(4), 575–580. doi: [10.1127/0935-1221/2007/0019-1741](https://doi.org/10.1127/0935-1221/2007/0019-1741).
- Sun HL, Zheng D. 1998. Formation, Evolution and Development of the Qinghai-Xizang Plateau. Guangzhou: Guangdong Science and Technology Press, 1–350 (in Chinese with English abstract).
- Swain B. 2016. Recovery and recycling of lithium: a review. *Separation & Purification Technology*, 172, 388–403. doi: [10.1016/j.seppur.2016.08.031](https://doi.org/10.1016/j.seppur.2016.08.031).
- USGS. 2019. Minerals commodity summaries: Lithium. Geological Survey: 1–2. <https://pubs.usgs.gov/periodicals/mcs2019/mcs2019-lithium.pdf>.
- USGS. 2020. Minerals commodity summaries: Lithium. Geological Survey: 1–2. <https://pubs.usgs.gov/periodicals/mcs2020/mcs2020-lithium.pdf>.
- USGS. 2021. Minerals commodity summaries: Lithium. Geological Survey: 1–2. <https://pubs.usgs.gov/periodicals/mcs2021/mcs2021-lithium.pdf>.
- USGS. 2022. Minerals commodity summaries: Lithium. Geological Survey: 1–2. <https://pubs.usgs.gov/periodicals/mcs2022/mcs2022-lithium.pdf>.
- USGS. 2023. Minerals commodity summaries: Lithium. Geological Survey: 1–2. <https://pubs.usgs.gov/periodicals/mcs2023/mcs2023-lithium.pdf>.
- Vine JD., Dooley JR. 1980. Where on Earth is all the lithium?; with a section on uranium isotope studies, Open-File Report 80-1234, USGS, 1–114. doi: [10.3133/ofr801234](https://doi.org/10.3133/ofr801234).
- Wang CG, Zheng MP. 2019. Hydrochemical Characteristics and Evolution of Hot Fluids in the Gudui Geothermal Field in Comei County, Himalayas. *Geothermics*, 81(SEP.), 243–258. doi: [10.1016/j.geothermics.2019.05.010](https://doi.org/10.1016/j.geothermics.2019.05.010).
- Wang DH, Dai HZ, Liu SB, Li JK, Wang CH, Lou DB, Yang YQ, Li P. 2022. New progress and trend in ten aspects of lithium exploration practice and theoretical research in China in the past decade. *Journal of Geomechanics*, 28(5), 743–764 (in Chinese with English abstract). doi: [10.12090/j.issn.1006-6616.20222811](https://doi.org/10.12090/j.issn.1006-6616.20222811).
- Wang DH, Li PG, Qu WJ, Lei ZY, Liao YC. 2013. Discovery and preliminary study of the high tungsten and lithium contents in the Dazhuyuan bauxite deposit, Guizhou, China. *Science China: Earth Sciences*, 56, 145–152 (in Chinese with English abstract). doi: [10.1007/s11430-012-4504-2](https://doi.org/10.1007/s11430-012-4504-2).
- Wang QS, Yuan CH, Xu H. 2015. Analysis of the global lithium resource distribution and potential. *China Mining Magazine*, 24(02), 10–17 (in Chinese with English abstract). doi: [10.3969/j.issn.1004-4051.2015.02.005](https://doi.org/10.3969/j.issn.1004-4051.2015.02.005).
- Wu XS, Huang WB, Du XH, Li L. 2014. Study on metallogenic types and models of lithium deposits in the world. *Deposit geology*, 33(S1), 1197–1198 (in Chinese with English abstract). doi: [10.16111/j.0258-7106.2014.s1.601](https://doi.org/10.16111/j.0258-7106.2014.s1.601).
- Xiao MS, Wang SH, Zhang QF, Zhang JW. 1997. Leaching mechanism of the spodumene sulphuric acid process. *Rare Metals*, 16(1), 37–45.
- Xu SS, Song JF, Bi QY, Chen Q, Zhang WM, Qian ZX, Zhang Lei, Xu SA, Tang N, He T. 2021. Extraction of lithium from Chinese salt-lake brines by membranes: Design and practice. *Journal of Membrane Science*, 635, 119441. doi: [10.1016/j.memsci.2021.119441](https://doi.org/10.1016/j.memsci.2021.119441).
- Yu F, Wang DH, Yu Y, Liu Z, Gao JQ, Zhong JA, Qin Y. 2019. The Distribution and Exploration Status of Domestic and Foreign Sedimentary-type Lithium Deposits. *Rock and Mineral Analysis*, 38(3), 354–364 (in Chinese with English abstract). doi: [10.15898/j.cnki.11-2131/td.201901180013](https://doi.org/10.15898/j.cnki.11-2131/td.201901180013).
- Zhang YL, Chen L, Wang KM, Wang G, Guo XQ, Nie X, Pang XY. 2022. Metallogenic characteristics of sedimentary lithium resources. *Mineral Deposits*, 41(05), 1073–1092 (in Chinese with English abstract). doi: [10.16111/j.0258-7106.2022.05.012](https://doi.org/10.16111/j.0258-7106.2022.05.012).
- Zhao L, Wang XB, Dai SF. 2022. Lithium resources in coal-bearing strata: Occurrence, mineralization and resource potential. *Journal of China Coal Society*, 47(05), 1750–1760 (in Chinese with English abstract). doi: [10.13225/j.cnki.jccs.MJ22.0418](https://doi.org/10.13225/j.cnki.jccs.MJ22.0418).
- Zhao YY, Fu JJ, Li Y. 2015. Super Large Lithium and Boron Deposit in Jadar Basin, Serbia. *Geological Review*, 61(01), 34–44 (in Chinese with English abstract). doi: [10.16509/j.georeview.2015.01.001](https://doi.org/10.16509/j.georeview.2015.01.001).
- Zheng MP, Chen WX, Qi W. 2016. New Findings and Perspective Analysis of Prospecting for Volcanic Sedimentary Boron Deposits in the Tibetan Plateau. *Acta Geoscientica Sinica*, 37(4), 407–418 (in Chinese with English abstract). doi: [10.3975/cagsb.2016.04.03](https://doi.org/10.3975/cagsb.2016.04.03).
- Zheng MP, Liu WG. 1987. A new lithium mineral-Zabuyeite. *Geological Review*, 79(4), 365–368 (in Chinese with English abstract).
- Zheng MP, Lü YY. 2018. The 'Nuclear Boron Ore' Viewed from the Angle of Geochemistry. *Acta Geoscientica Sinica*, (2), 250–256 (in Chinese with English abstract). doi: [10.3975/cagsb.2018.012301](https://doi.org/10.3975/cagsb.2018.012301).
- Zheng MP, Wang QX, Duo J. 1989a. A new type of hydrothermal deposit: cesium-bearing geysirite in Tibet. Beijing: Geological Publishing House, 1–114 (in Chinese with English abstract).
- Zheng MP, Xiang J, Wei XJ, Zheng Y. 1989b. Saline Lake on the Qinghai-Xizang (Tibet) Plateau. Beijing: Science Press, 1–431 (in Chinese with English Abstract).
- Zheng MP, Yuan HR, Liu JY, Li YH, Ma ZB, Sun Q. 2007. Sedimentary characteristics and paleoenvironmental records of Zabuye Salt Lake, Tibetan Plateau, since 128 ka BP. *Acta Geologica Sinica-English Edition*, 81(5), 861–874. doi: [10.1111/j.1755-6724.2007.tb01008.x](https://doi.org/10.1111/j.1755-6724.2007.tb01008.x).
- Zheng MP, Yuan HR, Zhao XT, Liu XF. 2006. The Quaternary Pan-lake (Overflow) period and Paleoclimate on the Qinghai-Tibet Plateau. *Acta Geologica Sinica*, 80(2), 169–180 (in Chinese with English abstract).
- Zheng MP. 1995. A new type of hydrothermal deposit cesium-bearing geysirite in Tibet. Beijing: Geological Publishing House, 1–114 (in Chinese with English abstract).